Steady-State Evaluation of a Multiple Cable Mooring by Discrete Parameter Techniques

by

R. F. Dominguez

R. W. Filmer

Civil Engineering Department
Oregon State University

BULLETIN NO. 46, AUGUST 1970
ENGINEERING EXPERIMENT STATION
OREGON STATE UNIVERSITY
CORVALLIS, OREGON

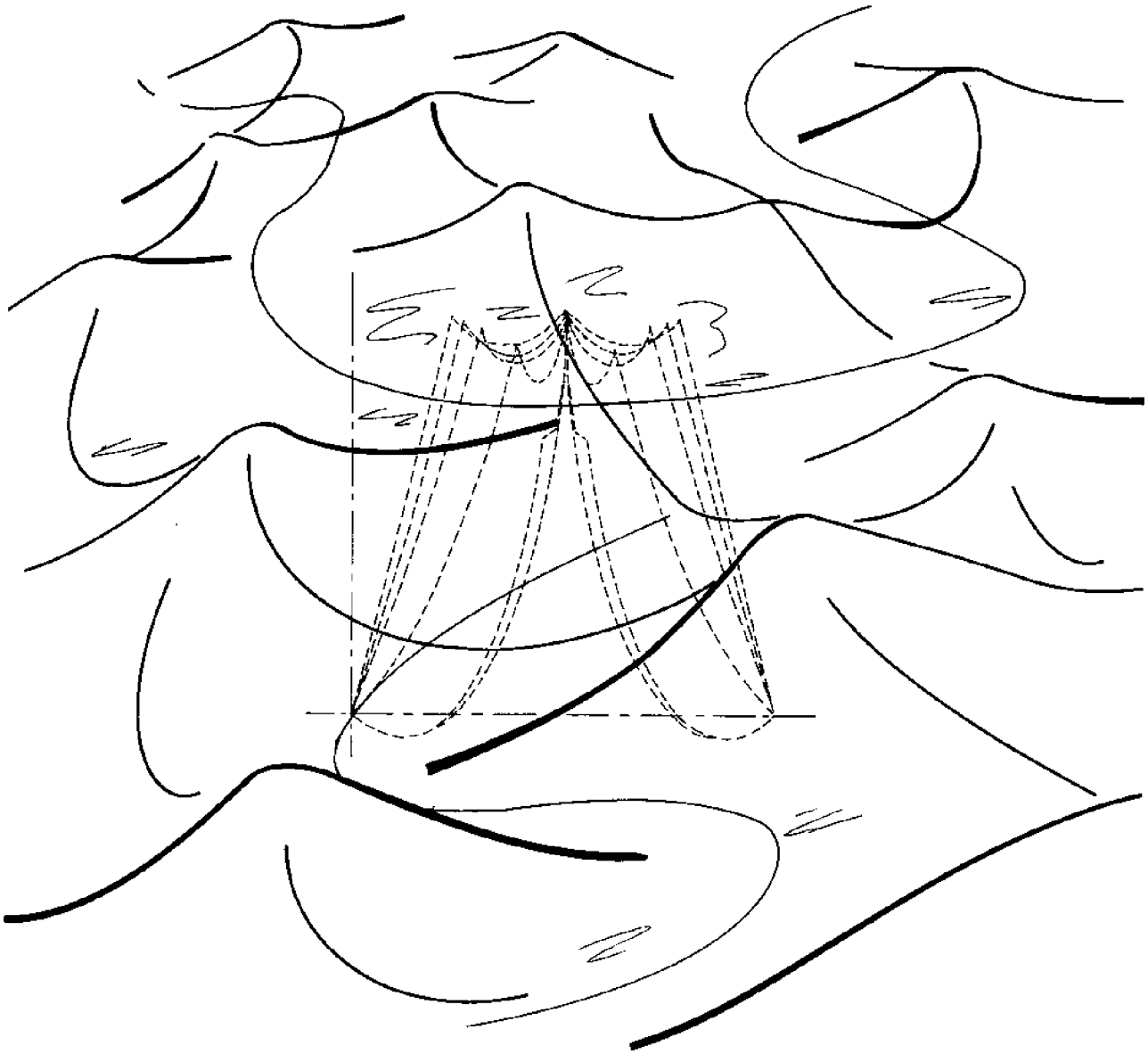

STEADY-STATE EVALUATION OF A MULTIPLE CABLE MOORING BY DISCRETE PARAMETER TECHNIQUES

by

R. F. Dominguez
R. W. Filmer

Civil Engineering Department
Oregon State University
Corvallis, Oregon 97331

BULLETIN NO. 46

AUGUST 1970

Supported in part by Oregon State University National Science Foundation Sea Grant-Institutional Grant GH-97.

Engineering Experiment Station
Oregon State University
Corvallis, Oregon 97331

ACKNOWLEDGMENTS

Partial support for this work was provided by the Oregon State University National Science Foundation Sea Grant-Institutional Grant GH-97.

Appreciation is extended to Mr. Jeffrey Sires for computer programming assistance and to Mr. Bruce Crist for assistance in the reduction and plotting of data. Thanks go also to Mrs. Bonnie Whitten who lettered the many figures. We also wish to thank Dr. John H. Nath and Dr. Steven Neshyba from whom the suggestion for the project originated and who maintained a very active interest in the research.

PREFACE

This bulletin deals only with the steady-state or static analysis of cable mooring systems and represents a portion of a much broader investigation which includes dynamic effects.

The complete analytical study, (Dominguez 1971) extends this static analysis technique to dynamic analysis using matrix methods. This makes it possible to obtain an eigenvalue solution. In reduced matrix form, the damped equations of motion are uncoupled by means of a linear transformation from the physical to a complex coordinate system, permitting evaluation of either characteristic or forced motion of cable systems.

Nomenclature

Symbols	Definition
A_i	A constant of integration
$\overline{A}$	Reaction force
$\mathbb{A}$	Aspect ratio
a	Catenary parameter
B_i	A constant of integration
$\overline{B}$	Reaction force
B_s	Net spring buoy buoyancy
D	Depth
d_s	Distance from the mean sea surface to the mooring connection on the surface buoy
C_d	Drag coefficient
$\mathbb{C}$	Compliancy number
E	Total closure error
E_b	Closure error at surface buoy
E_m	Closure error at right anchor position
F	Force
Fd	Hydrodynamic drag force
F_x, F_y, F_z	Force components in the x, y, z directions
h	Vertical distance between cable support positions
h_ℓ	Vertical height from the left support to the low point of cable
h_r	Vertical height from the right cable support to the low point of cable
i	Index
$\underline{i}, \underline{j}, \underline{k}$,	Orthogonal unit vectors
k	Surface buoy index
L	Cable length
$\mathbb{L}$	Dimensionless cable length ratio
$\overline{M}$	Moment vector
m	Mass
N	Horizontal coordinate interval used in program CATENARY

Symbols	Definition
P_i	A concentrated load
R_x, R_y, R_z	Reaction components in the x, y, z directions
$\bar{r}$	Position vector
$\bar{r}_w$	Position vector to the centroid of a distributed load
$	Spread ratio
s	Length measured along a cable
s^p, s^t	Cable segment components
T	Tension
T_x, T_y	Tension components
t	Time
v	Velocity
w	Uniformly distributed load
x	Orthogonal coordinate
x_ℓ	Horizontal distance from the left cable support to the low point of the cable for positive σ ratios
x'_ℓ	Horizontal distance from the left cable support to the low point in the cable for negative σ ratios
x_{rn}	Anchor span and right anchor coordinate
x_r	Horizontal distance from the right support, to the [illegible] point of cable
x_t	Cable span
y	Orthogonal coordinate
y_{rn}	Right anchor coordinate
z	Orthogonal coordinate
z_{rn}	Right anchor coordinate
f	Cable sag
Δ_t	Corrective force at surface buoy
$\Delta_x, \Delta_y, \Delta_z$	Corrective forces at right anchor position
δ	Positive correction value
ϵ	Termination test value used in Newton-Raphson [illegible]
θ	Horizontal surface force angle
κ	Convergence termination value
π	3.14159265
ρ	Fluid mass density
σ	Span to cable sag ratio; wave frequency
τ	Cable slope
φ	Horizontal velocity field angle

LIST OF FIGURES

TABLE OF CONTENTS

1. INTRODUCTION

1.1 General Introduction

The world today is faced with the growing problem of meeting current and projected needs of an expanding world population. As a result, attention is being focused upon the sea as a means of fulfilling requirements in the future. New and imaginative effort, coupled with increased scientific knowledge and technological capability, will be mandatory for intelligent and efficient utilization of the unfathomed resources of the ocean.

Traditionally, oceanographic exploration has followed a pattern of gathering data from ships in either single or cooperative ventures. Measurements taken at scattered geographic positions over long periods of time (often on the order of years) is costly and often an inadequate means for accumulating information necessary to the study of time dependent transport and circulational processes. Further exploration and development of marine resources will necessitate the construction of complex structural systems in deep water. Crucial to such development is the need to accurately predict wave conditions far in advance of their occurrence.

Regional or global systems of strategically dispersed remote

sensing buoys could provide a means for meeting these needs. Such systems would provide a capability for monitoring sea state and lower atmospheric conditions. By accumulating data they would provide information necessary for better understanding the basic phenomena involving the generation of wind waves, thereby leading to improved and reliable wave forecasting.

Oceanographical measurement from fixed positions has long been desirable, but to date only limitedly attainable. A major obstacle to the placement of such installations has been their unreliability and short life. The ocean, and in particular the interfacial region, presents a harsh physical and chemical environment. Past inadequacies are attributable to an insufficient backlog of both knowledge and experience in this environment, in relation to the behavior of materials, instruments and structural systems.

A long history of unsuccessful mooring attempts and the recent profusion of basic buoys and mooring schemes attests to the interest and need to develop this capacity. Causes traceable to mooring failures are diverse, ranging from component overstress to shark bite and corrosion. Structural failures resulting from inadequate design can be ascribed to a present inability to correctly predict the exact nature and extent of the forces which a mooring system will be required to withstand. Such forces are the result of complex static and dynamic interaction of both buoys and their moorings with lower

atmospheric winds, ocean waves and currents.

The ability to analyze a moored object and its cable mooring both statically and dynamically is essential for reliable structural and hydrodynamic design. Attempting to deal analytically with mooring problems can be discouraging when one reflects on the long years and substantial effort directed at evaluating hydro- and aerodynamic forces on rigid bodies, subject to steady flow. Analysis has yet to reach the point of exclusion of experimentation or reliance on empirically derived relations. Mooring problems involve fluid motion influenced by waves which have all the complexities of being non-uniform, non-steady, and turbulent. Detailed kinematic description of the flow field, involving both pressure and shear distribution on the buoy and cables is presently not possible. Flow conditions about a cable influenced by wave motion are complicated by the fact that the cable's trailing edge during one half cycle becomes its leading edge during the next, as the cable is accelerated back into its wake. The compliant nature of the cable further complicates the picture as it contributes to the relative motion by responding to variation in pressure along its length.

The static and dynamic behavior of flexible cables is also complex and not totally understood. Exact attainment of the static configuration under all but a few specific loadings is currently not possible.

A complete solution of the mooring behavior problem must

account for fluid structure interaction resulting from both waves and subsurface currents; structural and fluid energy dissipation, and elastic deformation of the systems' components must also be considered. In the case of some commonly used cable materials this effect can be appreciable and add still greater difficulty to the analysis, due to nonlinear stress-strain relationships (Wilson, 1967).

Approaches to the analysis of mooring systems have taken several directions. Attempts at analyzing the behavior of such systems by use of hydraulic models have been widely conducted. Experimental studies of large scale systems are, however, not without their difficulties. Facilities are normally limited in depth, necessitating the use of either small or partial models. Results obtained from such models tend to be of limited value. Cables which are on the order of several inches or less, in depths often approaching several thousand feet, present significant scaling difficulties. There appears to be a lack of comprehensive studies aimed at establishing model criteria required to properly evaluate the dynamical behavior of cable systems in fluids. Analytical attempts have been based on formulating equations of motion for the system and then attempting to arrive at solution under simplifying assumptions by various mathematical techniques. Other approaches have been based on the development of simplified system models and the adoption of both digital and analog computers.

The mooring behavior problem by its nature traverses many

areas of endeavor and engineering application. An extensive publication devoted entirely to reviewing the current status of analyzing cable systems under hydrodynamic loading has been written (Parsons and Casarella, 1969) to which the reader is referred for a comprehensive overview. Discussion of the results of other investigators will be undertaken in conjunction with either their usage or applicability to the material presented in subsequent sections of this study.

1.2. Background and Scope of Investigation

The use of large TOTEM spar buoys such as that shown in Figure 1.2-1 for data acquisition by Oregon State University's Department of Oceanography, necessitated the development of a reliable mooring technique capable of restraining the buoy while minimizing the vertical mooring reaction, as these buoys are limited in reserve buoyancy.

In view of this, a study was conducted (Dominguez, et al., 1969) to develop a mooring for installation of a TOTEM buoy in 1800 feet of water off the coast of Oregon. As a result the two-point mooring illustrated in Figure 1.3-1 was developed and later deployed. Its design was based on a necessarily limited amount of analytical work in conjunction with a structural analog to evaluate static behavior. Reliance was placed on a 1/100 scale model of the buoy and its mooring to evaluate the systems' response to directional waves. Static and

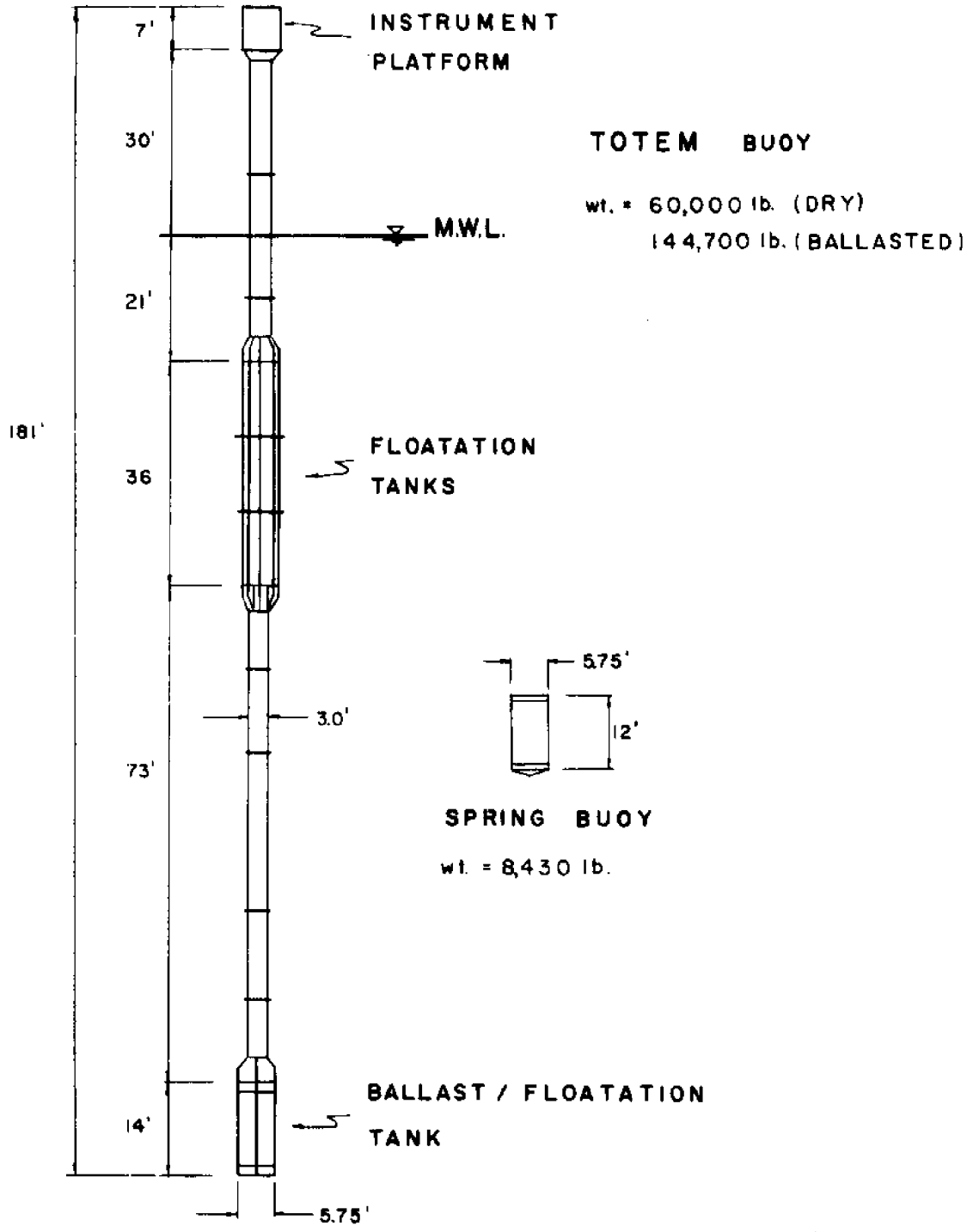

Figure 1.2-1 TOTEM OCEANOGRAPHIC SPAR BUOY

dynamic evaluation by these methods were limited with respect to depth. The static analysis was limited to two dimensions, neglecting hydrodynamic forces on the subsurface mooring components.

In view of the several drawbacks presented by such approaches to long term studies, it was felt that future development of such mooring systems required a capability of easily evaluating their behavior under a minimum number of restricting limitations. Hence the impetus for this study was provided.

The objectives of this study focus upon the development and application of numerical methods for statically analyzing discrete parameter represented moorings and cable systems, under generalized assumed known loadings.

1.3. Two-Point Mooring System

The two-point mooring system shown in Figure 1.3-1 consists of a set of anchors and a pair of subsurface spring buoys which provide support to a set of anchor and buoy connecting cables. When subject to external forces arising from either wind or current action on the surface buoy or subsurface components, a change in the mooring geometry must occur. The mooring can be thought of as being in a state of quasi-equilibrium dependent on cable generated forces to maintain its position. Under the influence of any external force the

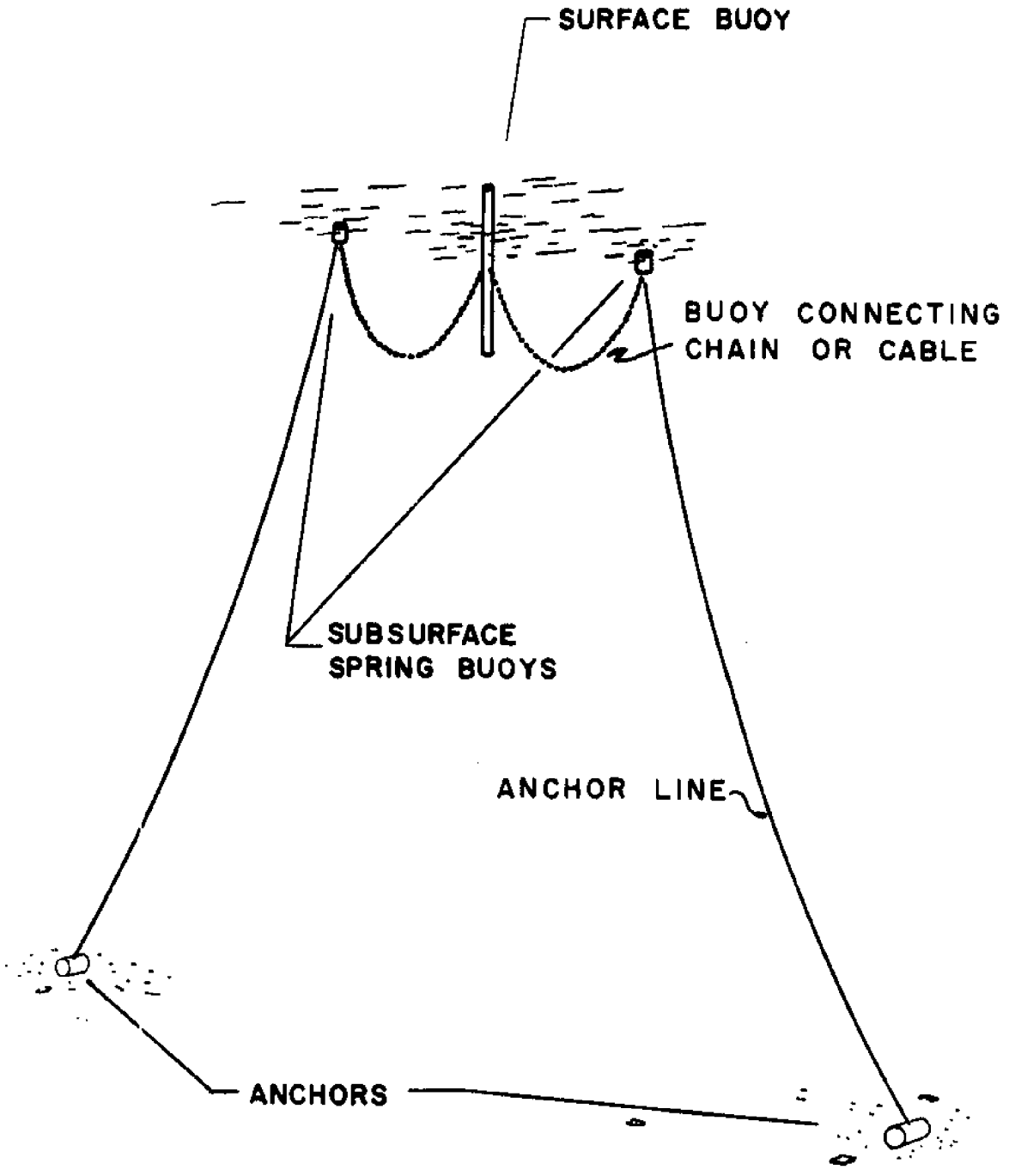

Figure 1.3-1 TWO-POINT MOORING SYSTEM

mooring must readjust and seek out a new equilibrium position compatible with the applied external forces and restraints on the system.

2. STATIC BEHAVIOR OF CABLE SYSTEMS

2.1. Statics of a Continuous Suspended Cable

Historically, the mathematical theory of flexible cables and chains has evolved under the assumption of total flexibility of the member. This assumption results in significant analytical simplification, as it implies that internal bending moments cannot be developed. Consequently internal shear forces cannot exist. Forces which a cable is then capable of transmitting are tensile forces only, and must be directed tangent to the cable at every point along its length.

The tangency requirement will be demonstrated, and equations developed, by considering the equilibrium of an elemental length of cable, following that given by Pestel and Thomson (1969).

Consideration of the element indicated in Figure 2.1-1 shows it to be acted upon by an external distributed load $w(s)$ whose resultant is $\overline{w}\Delta s$ and the internal cable reactions at either end of the element $\overline{T}$ and $\overline{T} + \Delta \overline{T}$. Equilibrium of the element requires that two conditions must be identically satisfied. The first may be expressed as

$$\Sigma \overline{F} = 0$$

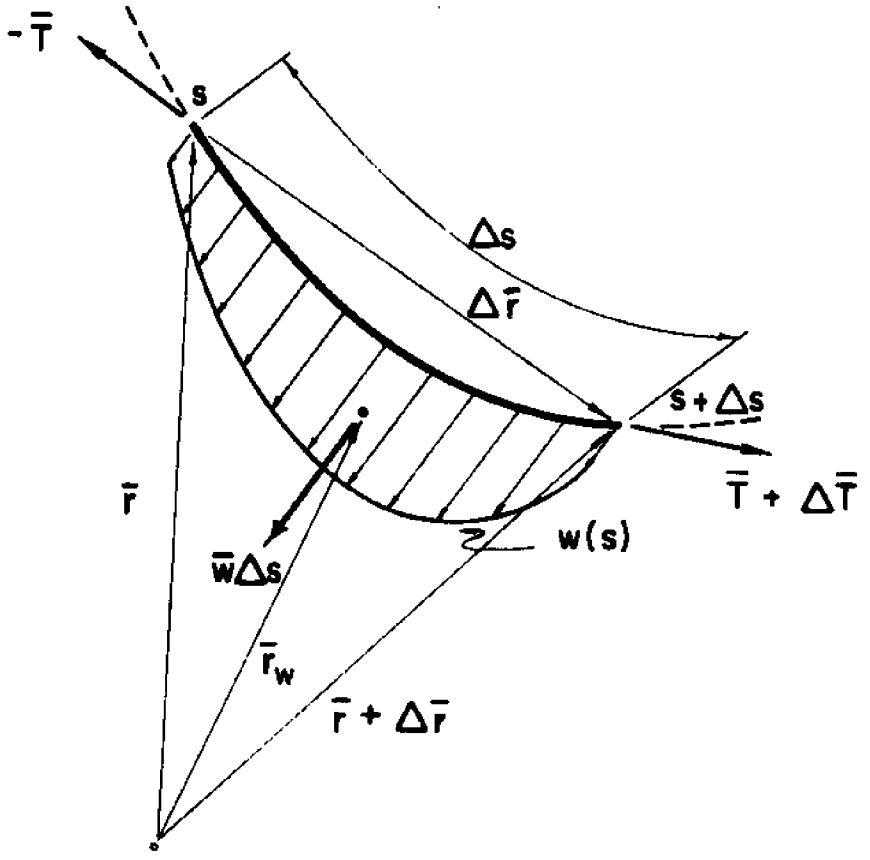

Figure 2.1-1 EQUILIBRIUM OF A CABLE ELEMENT, INFLUENCED BY AN EXTERNAL LOADING

where $\overline{F}$ = Force, external to the element. Applying this condition

$$-\overline{T} + (\overline{T} + \Delta\overline{T}) + \overline{w}\Delta s = 0$$

which reduces to

$$\frac{\Delta\overline{T}}{\Delta s} + \overline{w} = 0 \qquad (2.1\text{-}1)$$

Letting $\Delta s \to 0$, the following differential equation results,

$$\frac{d\overline{T}}{ds} + \overline{w} = 0 \qquad (2.1\text{-}2)$$

Application is now made of the second equilibrium condition which may be expressed as

$$\Sigma \overline{M}_0 = 0$$

where $\overline{M}$ = the moment produced by a force $\overline{F}$ about any arbitrary point 0. On substitution,

$$\overline{r} \times -\overline{T} + (\overline{r} + \Delta\overline{r}) \times (\overline{T} + \Delta\overline{T}) + \overline{r}_w \times \overline{w}\Delta s = 0$$

Expansion and division of this equation by Δs gives,

$$\overline{r} \times \frac{\Delta\overline{T}}{\Delta s} + \frac{\Delta\overline{r}}{\Delta s} \times \overline{T} + \frac{\Delta\overline{r}}{\Delta s} \times \Delta\overline{T} + \overline{r}_w \times \overline{w} = 0 \qquad (2.1\text{-}3)$$

Now if $\Delta s \to 0$, then $\Delta\overline{T} \to 0$ and $\overline{r}_w \to \overline{r}$, which gives

$$\overline{r} \times (\frac{d\overline{T}}{ds} + \overline{w}) + \frac{d\overline{r}}{ds} \times \overline{T} = 0 \qquad (2.1\text{-}4)$$

The bracketed portion of the left hand term is zero by Eq. (2.1-2); hence the following differential equation is obtained

$$\frac{d\bar{r}}{ds} \times \bar{T} = 0 \qquad (2.1\text{-}5)$$

Since $\frac{d\bar{r}}{ds}$ is everywhere tangent to the cable then the direction of $\bar{T}$ must be also, in order to satisfy Eq. (2.1-5).

Equations (2.1-2) and (2.1-5) are the basic differential equations describing the internal force distribution and deflection geometry of a suspended cable subject to a distributed loading.

2.2. Development of the Equations for Two-Dimensional Analysis of a Suspended Cable

Use will now be made of Eqs. (2.1-2) and (2.1-5) to develop the basic equations for static analysis of suspended cable members under the influence of a distributed loading. If the distributed load is restricted to lying in a vertical plane, as shown in Figure 2.2-1, then

$$\bar{w}(s) = w(s)\underline{j} \qquad (2.2\text{-}1)$$

where $\underline{i}$, $\underline{j}$, $\underline{k}$ are unit vectors in the x, y, z directions of a right hand cable coordinate system.

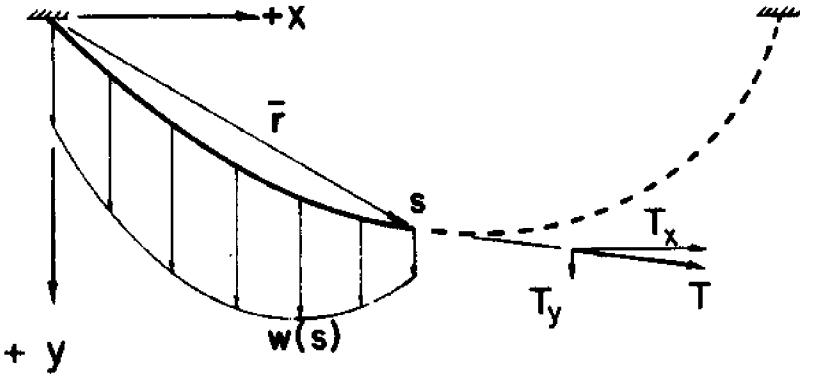

Figure 2.2-1 CABLE ACTED UPON BY A VERTICAL DISTRIBUTED LOADING

The internal tension force at any point s is thus

$$\bar{T} = T_x \underline{i} + T_y \underline{j} \tag{2.2-2}$$

Substituting Eq. (2.2-2) into Eq. (2.1-2) gives

$$\frac{dT_x}{ds} \underline{i} + \frac{dT_y}{ds} \underline{j} + w(s)\underline{j} = 0$$

Separating terms, one obtains

$$x: \quad \frac{dT_x}{ds} = 0 \tag{2.2-3}$$

$$y: \quad \frac{dT_y}{ds} + w(s) = 0 \tag{2.2-4}$$

Eq. (2.2-3) implies that everywhere in the cable the horizontal component of the tension force is constant. Integrating Eq. (2.2-4) will give

$$T_y = -\int w(s)ds + A_i \tag{2.2-5}$$

If the position vector $\bar{r}$ from the origin of coordinates to any point, located on the cable, at a distance s is expressed in rectangular Cartesian coordinates as

$$\bar{r} = x\underline{i} + y\underline{j}$$

and $\bar{r}$ is substituted into the second of the basic differential cable equations, then Eq. (2.1-5) gives

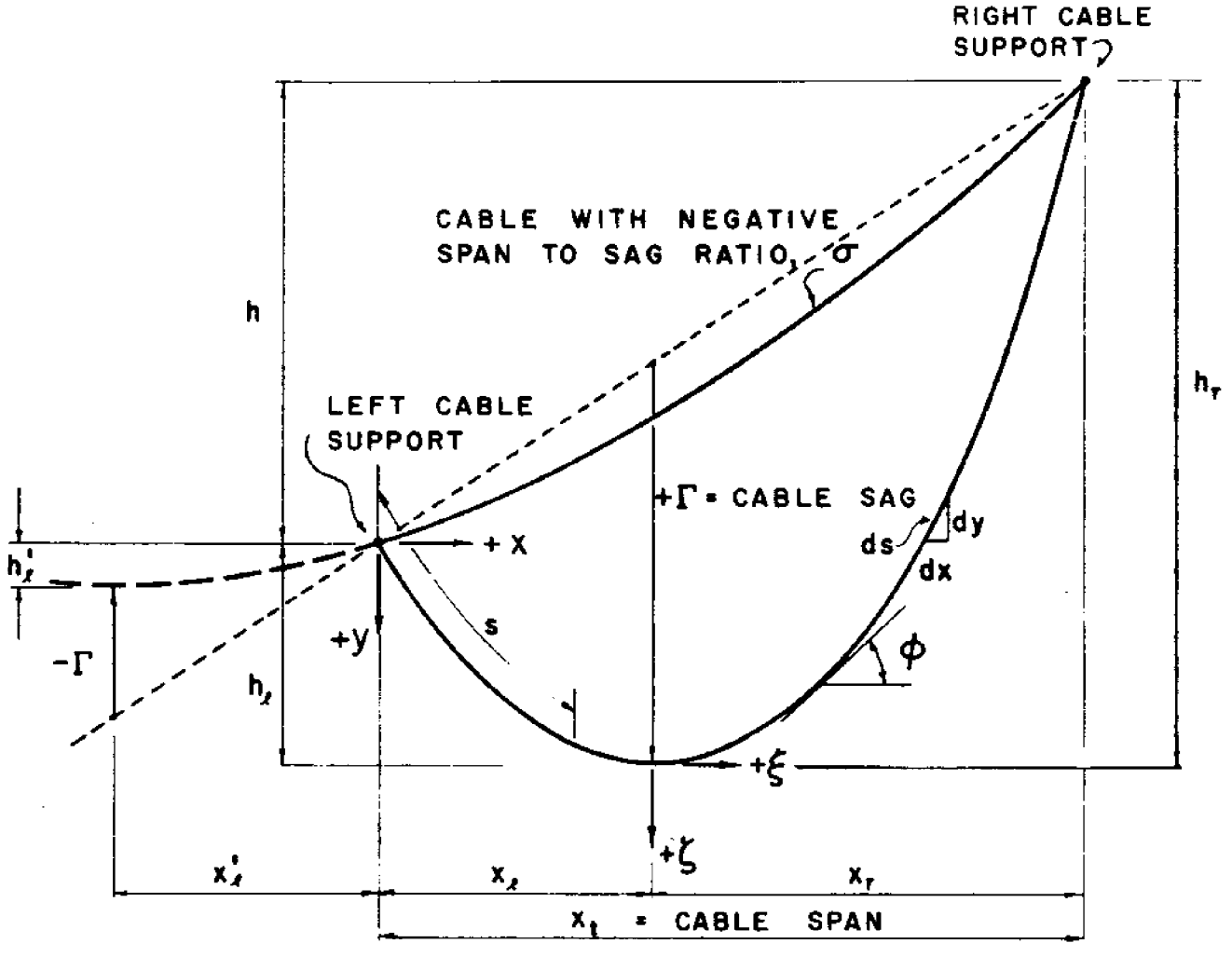

Figure 2.2-2 SUSPENDED CABLE NOMENCLATURE AND GEOMETERY

$$\left(\frac{dx}{ds}\underline{i} + \frac{dy}{ds}\underline{j}\right) \times \left(T_x\underline{i} + T_y\underline{j}\right) = 0$$

$$\frac{dx}{ds} T_y \underline{k} - \frac{dy}{ds} T_x \underline{k} = 0$$

$$T_y = T_x \frac{dy}{dx} \qquad (2.2\text{-}6)$$

Substitution of this last expression, Eq. (2.2-6) into Eq. (2.2-5) is now made, obtaining the following expression for the cable slope at any point.

$$\frac{dy}{dx} = -\frac{1}{T_x} \int w(s)ds + A_1 \qquad (2.2\text{-}7)$$

From Figure 2.2-2 the following geometrical relationship can be seen to exist:

$$\frac{dy}{dx} = \left[\left(\frac{ds}{dx}\right)^2 - 1\right]^{\frac{1}{2}} \qquad (2.2\text{-}8)$$

Using this, Eq. (2.2-7) may now be written in the following form

$$\frac{ds}{dx} = \sqrt{1 + \left[-\frac{1}{T_x} \int w(s)ds + A_1\right]^2}$$

which upon separation of the variables and integration gives

$$x = \int \frac{ds}{\sqrt{1 + \left[-\frac{1}{T_x} \int w(s)ds + A_1\right]^2}} + A_2 \qquad (2.2\text{-}9)$$

This last equation, Eq. (2.2-9), may in general be utilized to obtain an expression for the deflection relationship of the cable $y = y(x)$ provided that the necessary integration can be carried out. Pestel and Thomson (1969) point out that this is normally quite difficult. However, there are two special cases of practical importance for which a closed solution for the deflection curve can readily be obtained. These will now be considered.

Parabola

For the case when the load acting on the cable is a prescribed function of x, then

$$\bar{w}(x) = w(x)\,\underline{j} \qquad (2.2\text{-}10)$$

which will lead to the following form of Eq. (2.1-2)

$$\frac{d\bar{T}}{dx} + w(x) = 0 \qquad (2.2\text{-}11)$$

As was previously done, this can be expressed in Cartesian components to give

$$\frac{dT_x}{dx} = 0 \qquad (2.2\text{-}12)$$

$$\frac{dT_y}{dx} + w(x) = 0 \qquad (2.2\text{-}13)$$

Hence

$$T_x = \text{Constant} \qquad (2.2\text{-}14)$$

$$T_y = -\int w(x)\,dx + B_1 \qquad (2.2\text{-}15)$$

The tension force tangency requirement given by Eq. (2.2-6) may now be used with Eq. (2.2-15) to obtain the following expression for the slope of the cable :

$$\frac{dy}{dx} = -\frac{1}{T_x}\int w(x)\,dx + B_1 \qquad (2.2\text{-}16)$$

The deflection curve is then described by

$$y(x) = -\frac{1}{T_x}\int\left[\int w(x)dx\right]dx + B_1 x + B_2 \qquad (2.2\text{-}17)$$

If $w(x) = w$ = constant, then Eq. (2.2-17) is easily integrated, giving the parabolic form of the cable deflection equation.

$$y(x) = -\frac{wx^2}{2T_x} + B_1 x + B_2 \qquad (2.2\text{-}18)$$

The integration constants in the above equations are evaluated by use of known boundary values, obtained from the physical constraints imposed on the problem, such as, specification of cable support locations, maximum deflection, or cable length. An important condition is that at the lowest point in the cable $\frac{dy}{dx} = 0$ which can be applied through use of Eq. (2.2-16).

Catenary

As pointed out, Eq. (2.2-9) may be utilized to obtain an expression describing the cable deflection curve. Consideration is now given to the important case where $w(s) = w = \text{constant}$ which corresponds to a uniform cable supporting its own weight. This relation may be derived by employing a coordinate system located at the end of the cable, as done by O'Brien and Francis (1964). However, in order to facilitate development and obtain less cumbersome results, a shift in coordinate system will be introduced, locating the new axes at the lowest point of the cable, as shown in Figure 2.2-2. At this point, the cable slope $\frac{dy}{dx} = 0$, $s = 0$, and $\xi = x - x_\ell = 0$. Application of the integrated form of Eq. (2.2-7) gives $A_1 = 0$. Eq. (2.2-9) then gives

$$\xi = \int \frac{ds}{\sqrt{1 + \left(\frac{ws}{T_x}\right)^2}} + A_2 \qquad (2.2\text{-}19)$$

which upon integration is

$$\xi = \frac{T_x}{w} \sinh^{-1} \frac{ws}{T_x} + A_2 \qquad (2.2\text{-}20)$$

At $\xi = 0$, $\zeta = 0$, $s = 0$, the constant $A_2 = 0$. Hence

$$\frac{ws}{T_x} = \sinh \frac{w\xi}{T_x} \qquad (2.2\text{-}21)$$

Integrating Eq. (2.2-7) with $A_1 = 0$, and then substituting Eq. (2.2-21)

into the result, gives

$$\frac{dy}{dx} = - \sinh \frac{w\xi}{T_x} \qquad (2.2\text{-}22)$$

Making the substitution $a = \frac{T_x}{w}$ and then integrating the above equation, one obtains

$$y = -a \cosh \frac{\xi}{a} + A_3 \qquad (2.2\text{-}23)$$

If the values $\xi = 0$ and $y = h_\ell$ at the transformed coordinate origin are substituted into the above equation then $A_3 = h_\ell + a$. Substituting this value of A_3 into Eq. (2.2-23) gives the catenary form of the cable deflection expression

$$y - h_\ell = -\frac{T_x}{w}\left[\cosh \frac{w(x-x_\ell)}{T_x} - 1\right] \qquad (2.2\text{-}24)$$

Since this equation contains three unknown values, h_ℓ, x_ℓ, and T_x additional relations are needed in order to make use of it. These can be obtained by evaluating Eq. (2.2-24) twice, at $x = 0$ and at $x = x_t = x_\ell + x_r$ and then subtracting the results leading to the following expression for h, the vertical distance between cable supports.

$$h = 2a \sinh \frac{x_t}{2a} \sinh \frac{2x_\ell - x_t}{2a} \qquad (2.2\text{-}25)$$

To obtain an expression for the length of the catenary L in terms of the cable span, one can integrate the following expression using Eq. (2.2-22) for $\frac{dy}{dx}$

$$L = \int_0^{x_t} \sqrt{1 + \left(\frac{dy}{dx}\right)^2}\, dx \qquad (2.2\text{-}26)$$

which after integration and the use of a hyperbolic identity gives

$$L = 2a \sinh \frac{x_t}{2a} \cosh \frac{2x_\ell - x_t}{2a} \qquad (2.2\text{-}27)$$

If both Eq. (2.2-25) and Eq. (2.2-27) are squared and then subtracted the following transcendental equation for the catenary parameter a is obtained.

$$\sinh \frac{x_t}{2a} = \frac{1}{2a} \sqrt{L^2 - h^2} \qquad (2.2\text{-}28)$$

In order to obtain equations which can be used easily to obtain the coordinates of the lowest position of the catenary in terms of the normally known parameters L, x_t and h, Eq. (2.2-25) and Eq. (2.2-27) may be combined to give

$$x_\ell = a \tanh^{-1} \frac{h}{L} + \frac{x_t}{2} \qquad (2.2\text{-}29)$$

A relation for the vertical coordinate h_ℓ may now be obtained by substituting Eq. (2.2-28) and Eq. (2.2-29) into Eq. (2.2-24) and evaluating the result at $x = 0$, $y = 0$, thus

$$h_\ell = a \left[\cosh \frac{x_\ell}{a} - 1\right] \qquad (2.2\text{-}30)$$

An expression for the tension at any point in the cable may now be obtained by combining Eqs. (2.2-2) and (2.2-6) with Eq. (2.2-22)

which describes the cable slope $\frac{dy}{dx}$ to give

$$T = aw \left[1 + \left(\sinh \frac{x - x_\ell}{a}\right)^2\right]^{\frac{1}{2}} \qquad (2.2\text{-}31)$$

2.3. Computer Program for Solution of Catenary Equations

Solving the equations governing the catenary geometry and internal force distribution necessitates the tedious solution of a rather complex set of hyperbolic equations, including a transcendental equation defining the catenary parameter. In view of this, a computer program was developed which provides a complete static solution by solving the equations presented in Section 2.2 based on the location of cable support positions, cable length and weight. This program, as were all programs used in this study, was written in Fortran IV for use with the Oregon State CDC 3300 computer facility, using the OS3 version 2.1 time sharing system.

The program incorporates a Newton-Raphson method for solving the transcendental equation, Eq. (2.2-28) which is first rearranged by transposition to obtain the form $F(a) = 0$.

$$\sinh \frac{x_t}{2a} - \frac{1}{2a}\sqrt{L^2 - h^2} = 0$$

Obtaining the root or the value of the catenary parameter a which satisfies this equation is accomplished by use of the recursion relation

$$a_{i+1} = a_i - \frac{F(a_i)}{F'(a_i)} \qquad (2.3\text{-}1)$$

where $F'(a_i)$ denotes the derivative of $F(a)$ with respect to a and evaluated at $a = a_i$.

Eq. (2.3-1) is used to obtain successive approximations to the value of a which will satisfy $F(a) = 0$. Successive approximations of a root are carried out until the value of $\frac{F(a_i)}{F'(a_i)}$ is less than some prescribed value ϵ, at which point the root satisfying the catenary parameter equation has been found. A flow chart illustrating the calculation sequence is given in Figure 2.3-1.

Subsequent figures relating to the catenary properties were developed using this program. Presented in Figure 2.3-2 is a dimensionless plot of the catenary parameter a illustrating its dependence on h, x_t and L for the range of configurations of interest. As this figure shows, the parameter has a wide range of values exhibiting very large changes as the span to length ratio approaches its asymptotic limit. As a approaches infinity, so must the cable tension. For deep catenaries with small positive span to sag ratios, the catenary parameter assumes a much narrower range of variation.

It was found that the Newton-Raphson criteria used for convergence in obtaining a proved to be direct and rapid for the range of $\frac{x_t}{L}$ above approximately 0.35. For lower ranges initial values had to be selected with greater care. Where initial values of a were

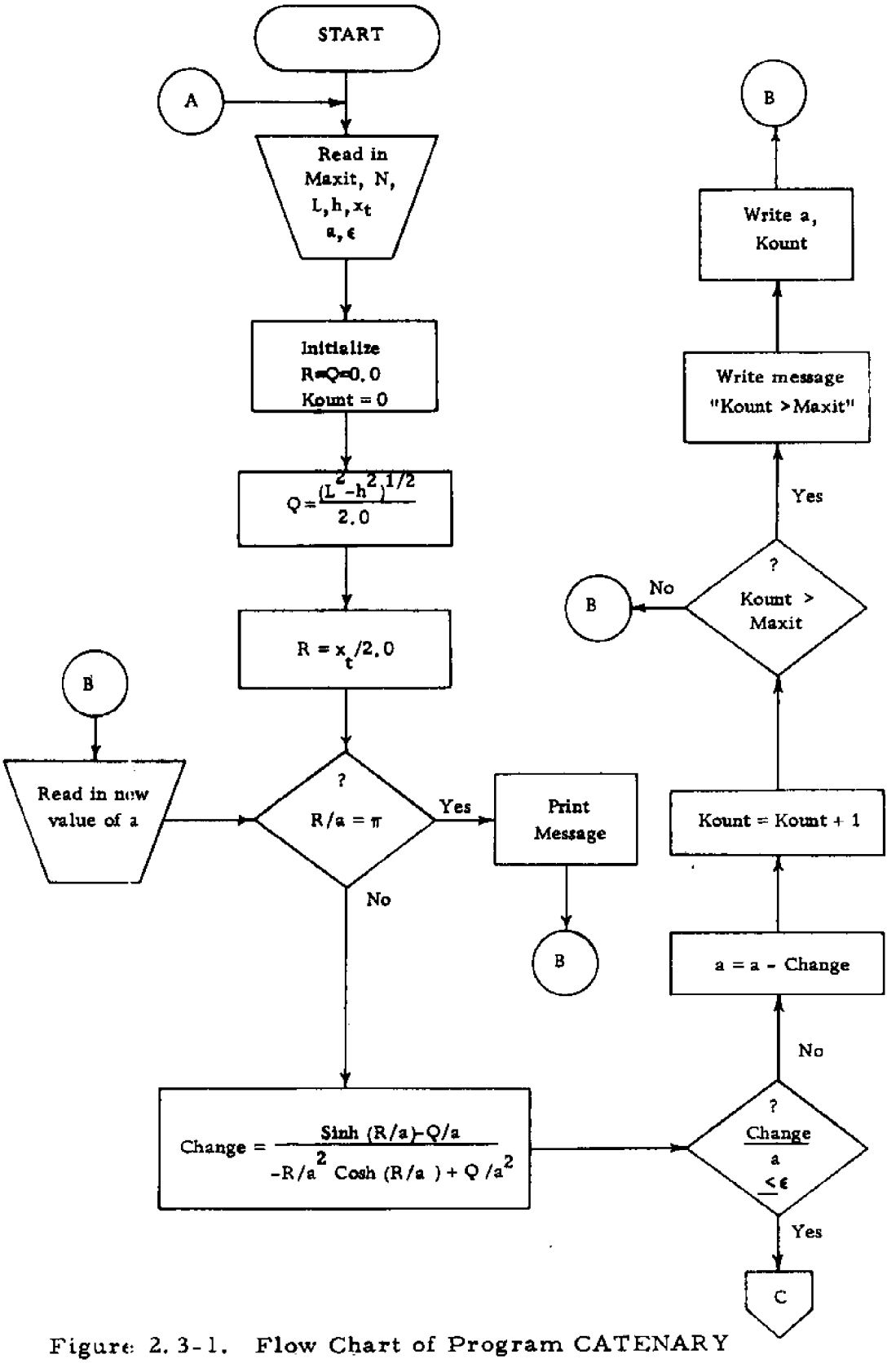

Figure 2.3-1. Flow Chart of Program CATENARY

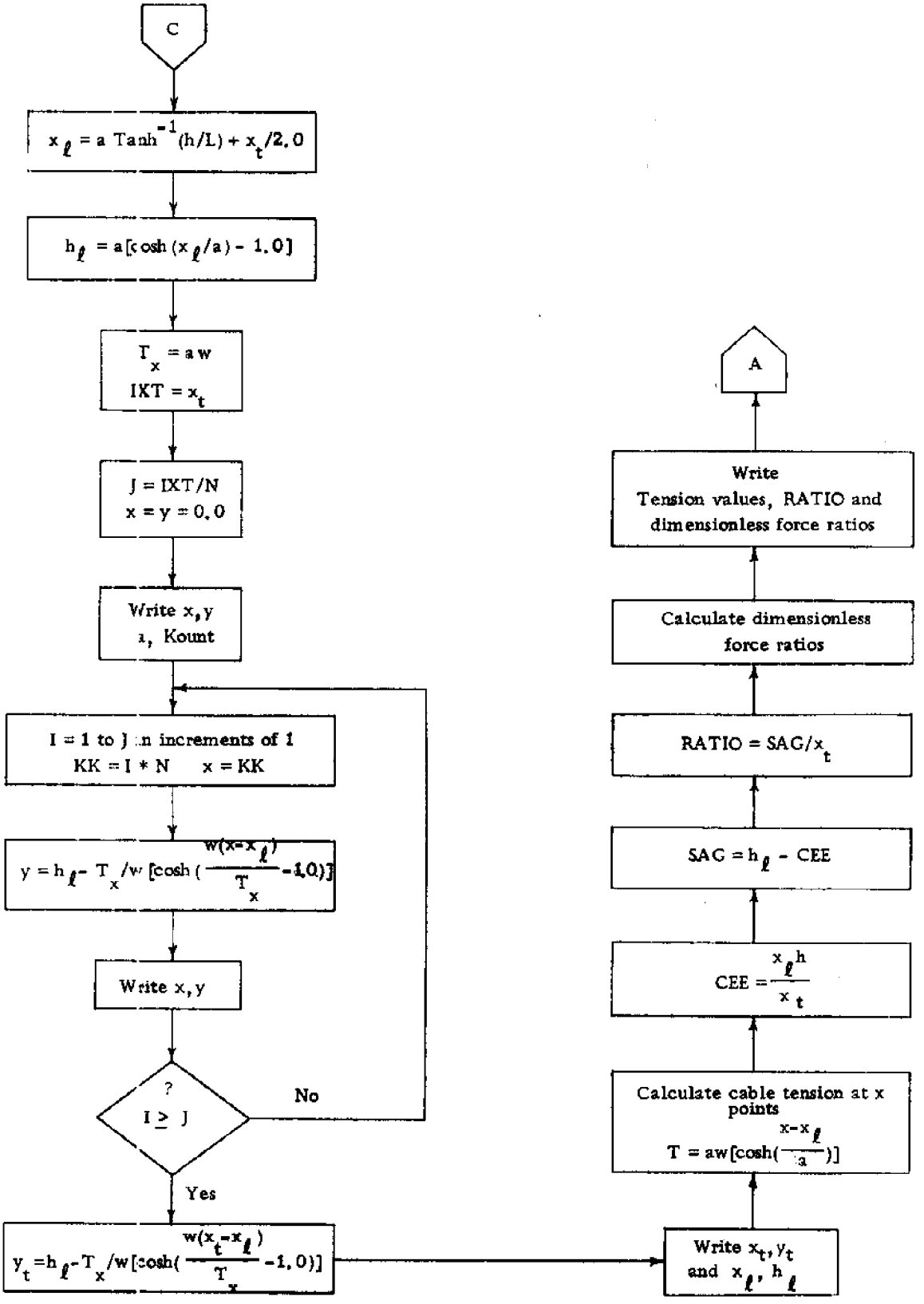

Figure 2.3-1 (continued)

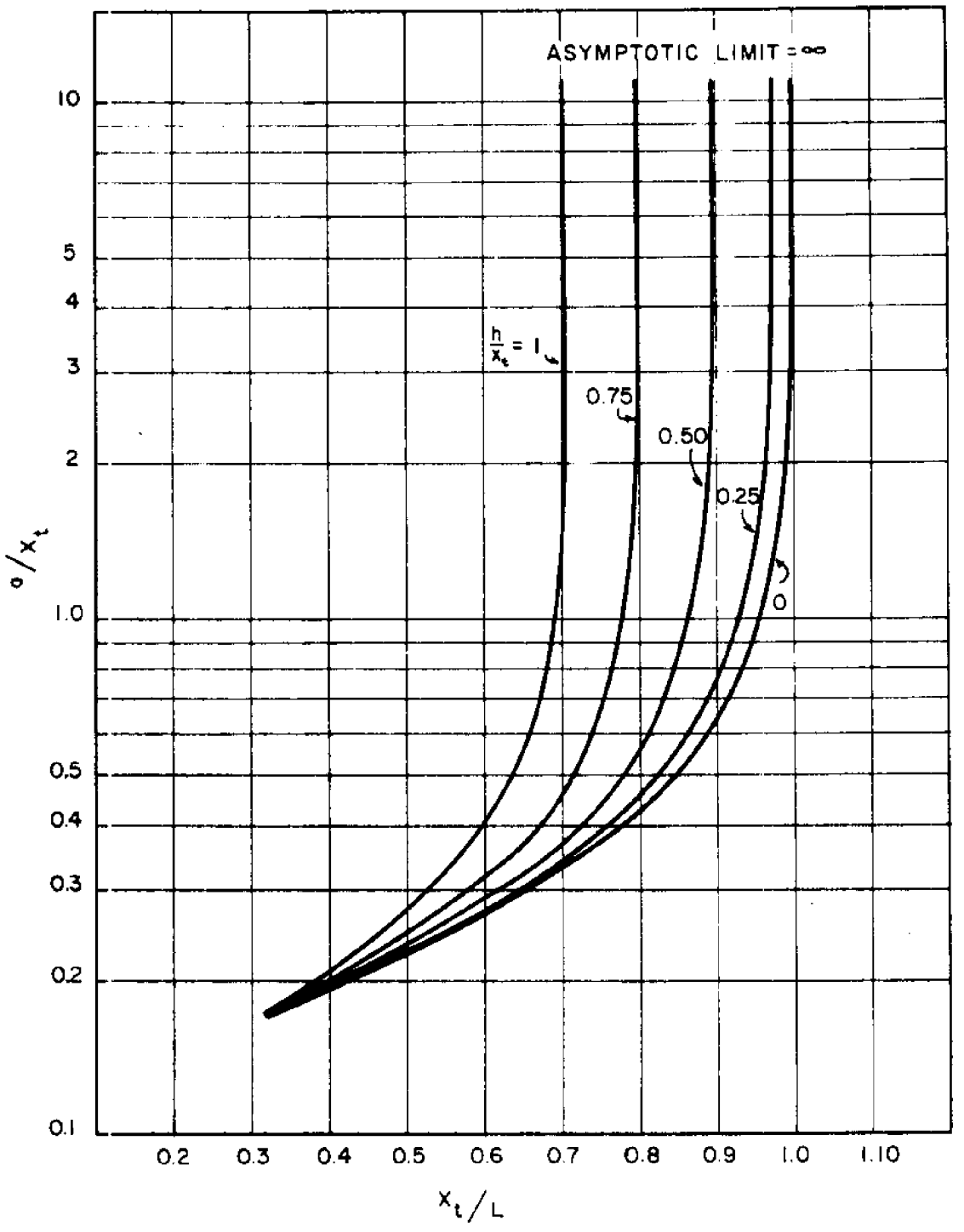

Figure 2.3-2 CATENARY PARAMETER DEPENDENCE ON X_t, L, AND h.

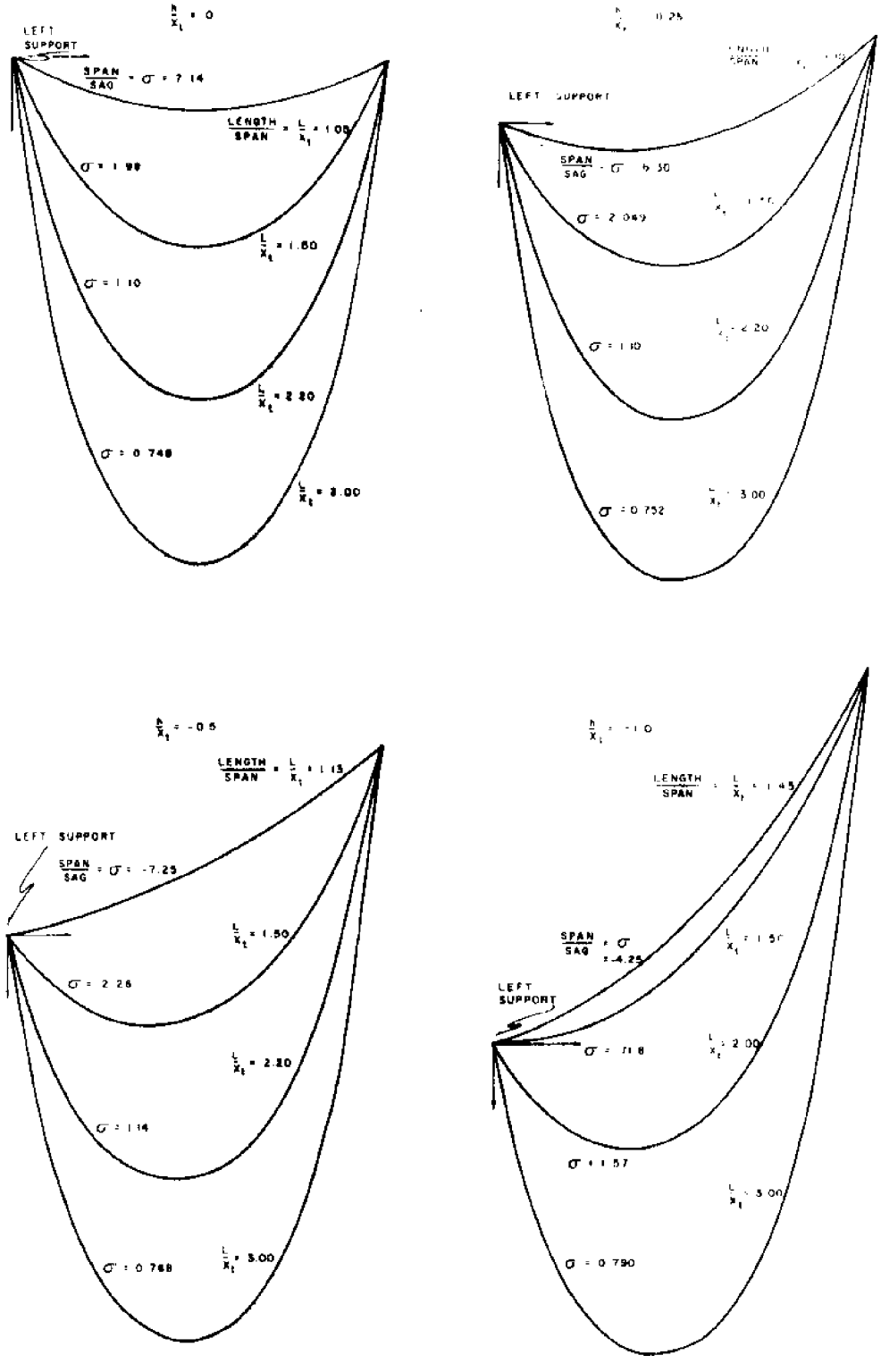

Figure 2.3-3 CATENARY CONFIGURATIONS, RELATIVE TO CABLE PARAMETERS

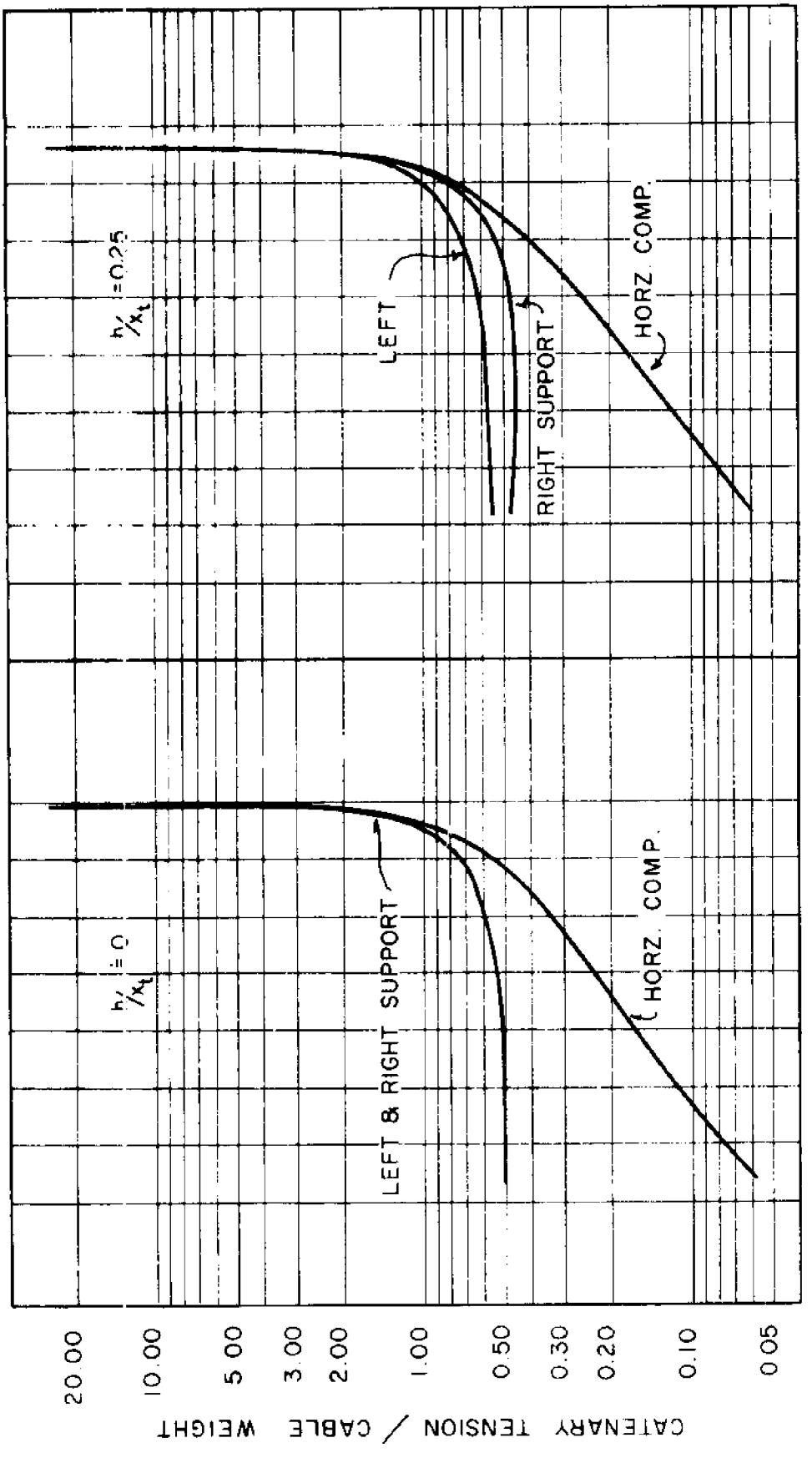

Figure 2 3-4 DIMENSIONLESS CATENARY TENSION VALUES FOR DIFFERING h/x_t RATIOS

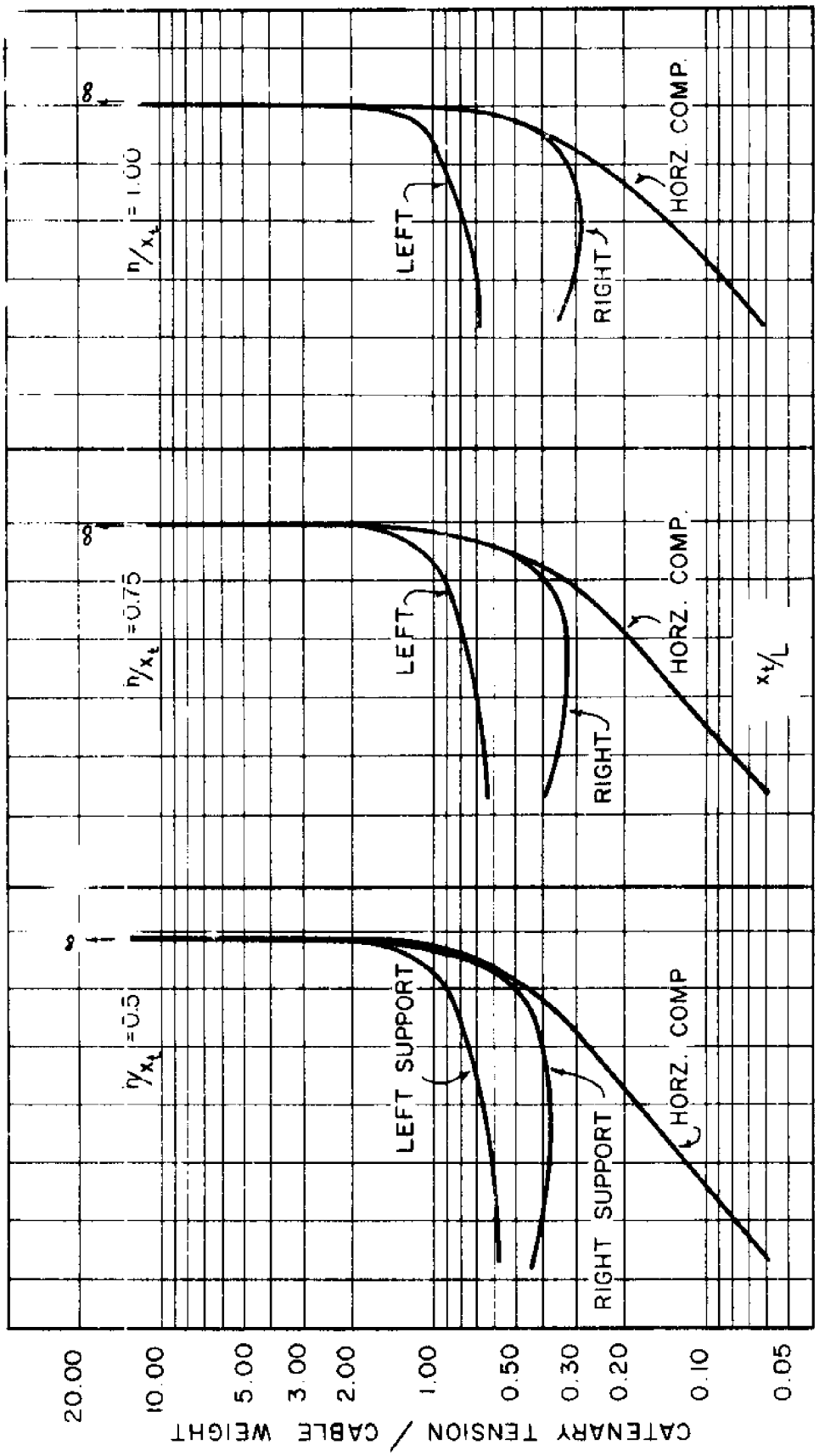

Figure 2.3-5 DIMENSIONLESS CATENARY TENSION VALUES FOR DIFFERING h/x_t RATIOS

within reasonable range of the correct value, convergence to ϵ, equal to or less than 0.0001, normally took place within four or five iterations.

In order to lend added geometric meaning to the parameters used in defining cable properties and configurations, Figure 2.3-3 is presented showing the catenary shapes as a function of the cable support position h, span to length ratio $\frac{x_t}{L}$ and the span to sag ratio $\sigma = \frac{x_t}{T}$. Figure 2.3-4 and Figure 2.3-5 show the cable tension dependence on catenary geometry and exemplify the non-linear nature of the static cable analysis problem. Variation of tension with increasing $\frac{x_t}{L}$ corresponds to the effect produced by forcing the cable support positions apart.

2.4. Analysis of Cable Systems

Cables have been used as load supporting members in such traditional structures as suspension bridges, tramways, transmission lines, etc. for some time. In recent years the application of cables to the construction of complex suspended roof systems has increased. As a consequence, behavioral theory and techniques for analysis of such structures have received a good deal of attention and are well documented (see Shore, 1969). In the case of such structural applications as these, support locations are known and are not a function of the systems' loading. Only small changes due to elastic deformation and temperature occur, which can be accounted for. Loading is

generally such that analysis can be carried out in a plane. For cables having relatively flat deflection curves the simpler parabolic form of the cable equations can be satisfactorily utilized, giving a good approximation to the exact case described by the catenary. In this case $\cos \phi \approx 1$, where ϕ is the cable slope measured from the horizontal (Figure 2.2-2). When ϕ is small everywhere, a good approximation of cable weight being distributed uniformly in the horizontal direction, is obtained. For cable systems which are subject to more complex loading (combinations of concentrated loads; discontinuous and non-uniformly distributed loads) deflection relations cannot in general be directly obtained by existing theory.

The equilibrium of all structures requires that the vector addition of all forces acting on it form a closed polygon. Analysis of beams, arches, and trusses, either graphic or algebraic, can be carried out on this basis. The procedure is well documented in books dealing with structural analysis and mechanics such as Michalos and Wilson (1965). The polygon principle can be extended to cable analysis when treated as a system acted upon by concentrated loads.

Approximate solution can be realized by use of the string polygon method, approximating hanging cables by a series of frictionless pin-connected, rigid but weightless segments. Loads including cable weight are replaced by equivalent concentrated forces located at the connecting node points. This results in a configuration which

is statically determinate and requires no prior assumption as to its geometric shape.

Existing cable theory can be applied to mooring systems provided the support positions are known and hydrodynamic drag forces are either non-existent or negligible. The catenary equations would then be applicable. However in the case of mooring applications, at least one of the cable supports is partially free to move, making its position a function of the systems' loading. In such a case the catenary relations are not applicable. Hydrodynamic forces acting on the cable cause it to assume a configuration that is no longer a catenary and in general does not lie in a plane. Consequently the geometric configuration may be three-dimensional.

This situation is exemplified by the analytical problem confronted in arriving at the static configuration of the two-point mooring system, under a generalized loading, illustrated in Figure 2.4-1. There are, as yet, no adequate analytical techniques for arriving at exact solutions to such problems. Although solutions for particular problems have been developed, no general method of analysis is available. Hanging cables are subject to large displacements and the differential equations describing their equilibrium are non-linear. This has excluded the application of methods based on linear superposition used in structural mechanics for the analysis of complex statically indeterminate structures.

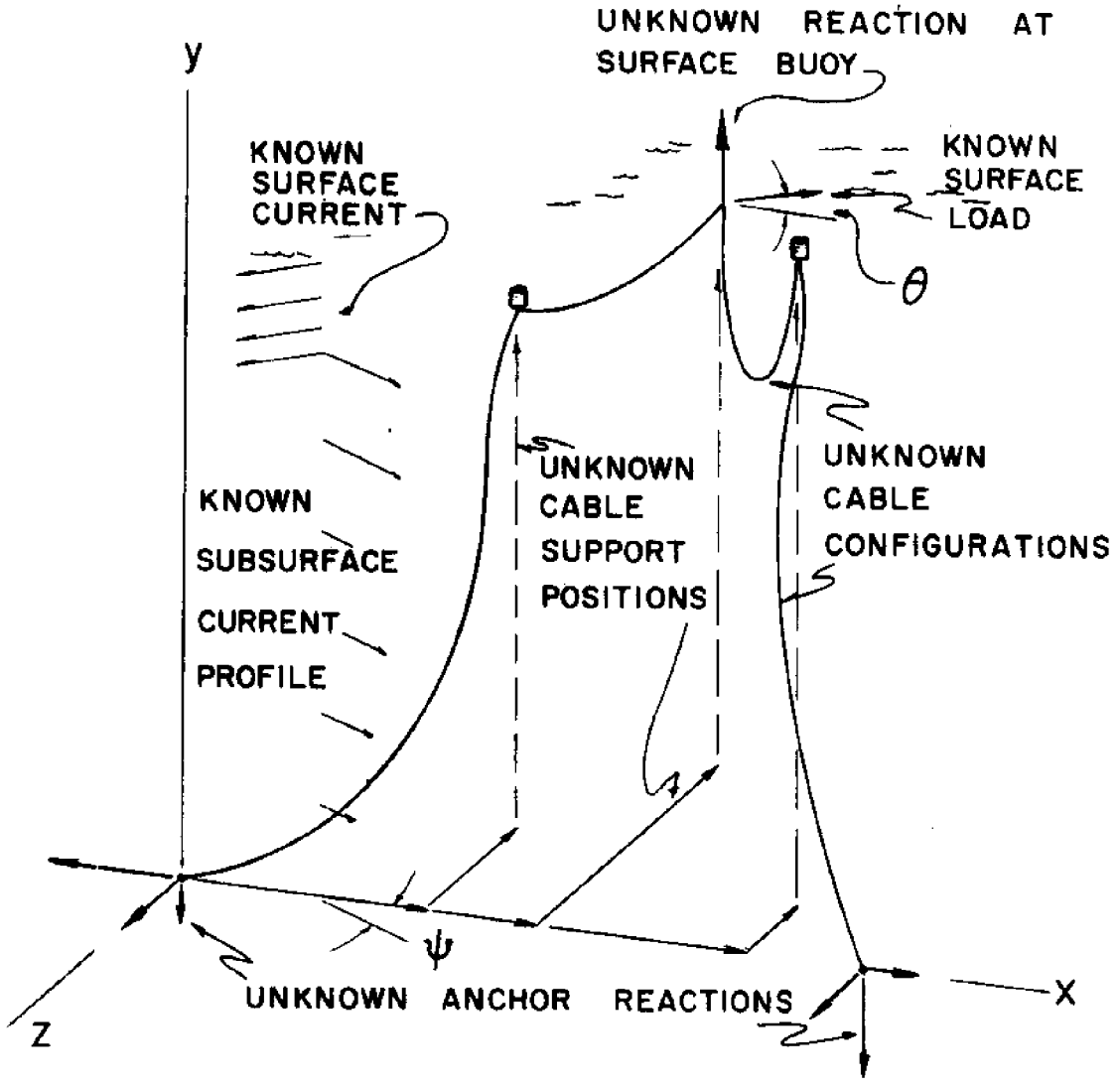

Figure 2.4-1 TWO-POINT MOORING UNDER A GENERALIZED 3-DIMENSIONAL LOADING

O'Brien and Francis (1964) set forth a numerical method for the two-dimensional analysis of cables by a process of successive approximations. This approach treats cable elements between concentrated loads as piecewise continuous catenaries, by applying the basic catenary relations to each segment of the cable between concentrated load points. Later O'Brien (1967) extended this technique to three-dimensional application and reportedly applied it to the design of deep sea moorings. Apparently motivated by O'Brien, Skop and O'Hara (1969) formalized the string polygon technique and applied it to three-dimensional cable arrays.

2.5. Basis of Numerical Solution Procedure

Based on the concepts put forth in the original paper by Skop and O'Hara, two numerical computer programs were developed to attain static solution of the two-point mooring and single cable systems.

In order to make clear the principle upon which the numerical solution procedure is based, it will first be explained by application to the simpler single cable.

Figure 2.5-1 shows a uniform cable, of known length L, suspended between supports a and b whose position is presumed known. In the absence of externally applied loadings, the cable shape would be described by the catenary relations previously developed.

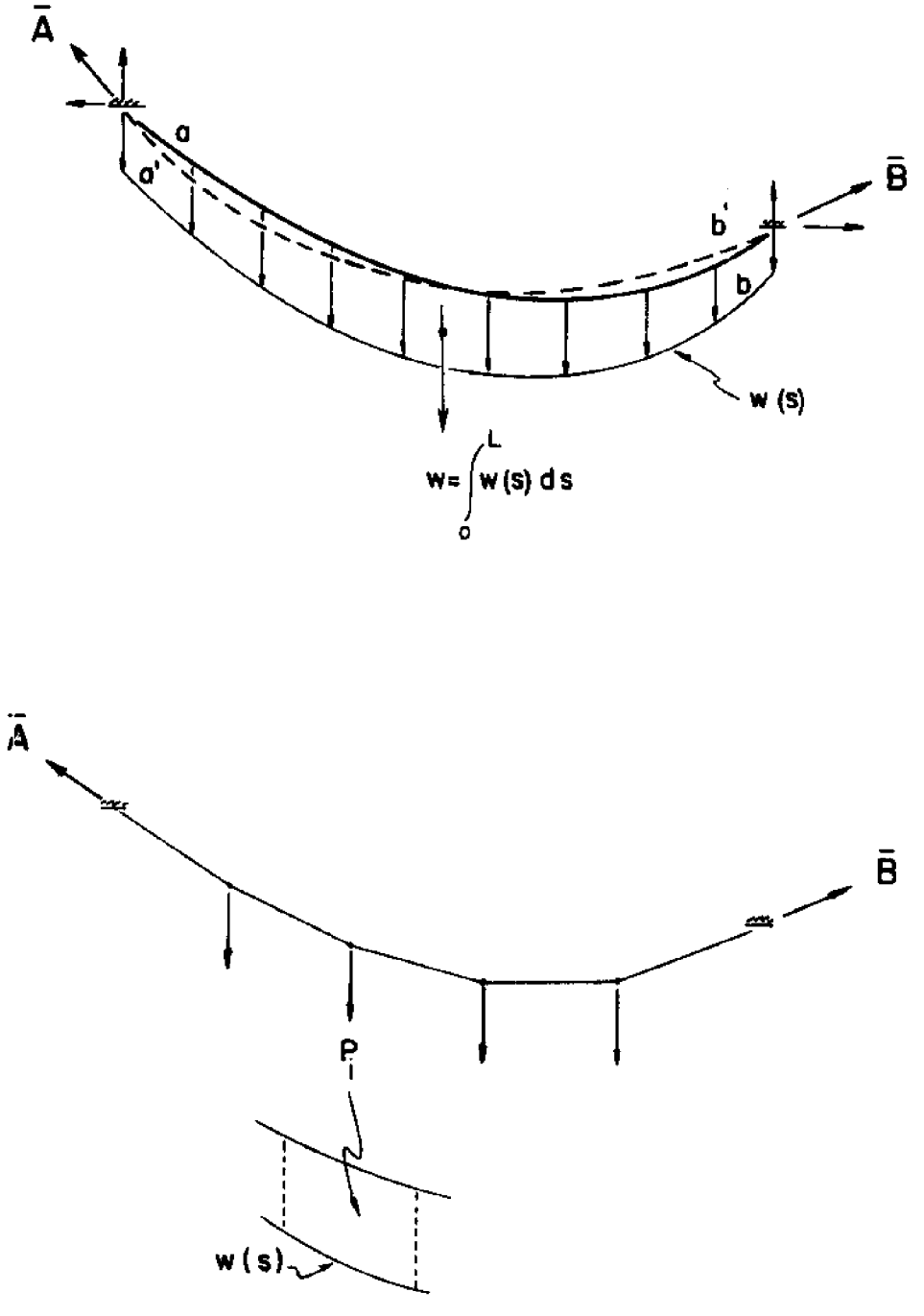

Figure 2.5-1 DISCRETE PARAMETER REPRESENTATION OF A CONTINUUM CABLE

Use of these could be made to determine the reactions $\overline{A}$ and $\overline{B}$ at the supports.

Suppose the cable is now subject to a distributed but arbitrary known loading w(s). Under this influence it deforms from its initial shape a-b to some other unknown configuration a'-b', shown dotted. Since w(s) is assumed known, the magnitude of its resultant can be determined by integrating the load along the cable length. As constituted, there are more unknowns than available independent equations, rendering the cable statically indeterminate. Though the magnitude of the resultant of the distributed load is determinable, its point of application is not, as a deflection relationship for the cable is unavailable. Since there are only three available equilibrium equations, other relations are needed to achieve a static solution. Knowledge of the deflected shape of the cable would remove a sufficient number of unknowns to render the problem statically determinable.

In order to surmount these difficulties, we approximate the original distributed system by a discrete or lumped parameter one (Figure 2.5-1), by dividing the cable into a stipulated number of segments such that the sum of their lengths equals the original cable length. The distributed load, including the cable weight acting on each segment, is replaced by an equivalent concentrated node point load. The unknown quantities are now: the magnitude of the reactions $\overline{A}$ and $\overline{B}$, their directions and the unknown positions of each

of the node points.

It would appear that this new system has increased the number of unknown quantities by virtue of each interior node point position being unknown at the outset. What has been accomplished is the replacement of an infinite number of unknown cable positions by a finite number of node points, each of which is accompanied by an independent set of equilibrium equations. In the discrete case, or polygon formulation, the support reactions as well as their directions are unknown.

Suppose for the moment that we free the cable at point b and select the unknown reaction $\overline{B}$ equal to its correct value. $\overline{A}$ can readily be calculated in terms of $\overline{B}$ by equating all external forces acting on the cable in the x and y directions to zero. Alternatively we could begin at point b and progress from connection to connection by considering the equilibrium of each individual segment. As the weight and external loading are applied at the node points, each cable segment is a two force member. Consequently, the resultant of all forces external to each segment must be colinear, equal and opposite. Application of this elementary principle of statics allows for the calculation of $\overline{A}$ in terms of $\overline{B}$ by successive calculation of internal reactions at all intervening node points.

This forms the basis upon which the numerical solution is formulated. Since the value of the redundant reaction $\overline{B}$ is not

known, a reasonable value is assumed. Then, beginning at point b, $\Sigma F_x = 0$ and $\Sigma F_y = 0$ are applied, evaluating in succession the internal cable reactions until point a is reached and $\bar{A}$ calculated in terms of the presumed value $\bar{B}$. At this stage all internal reactions in terms of $\bar{B}$ and the external cable loading have been evaluated. Use is now made of the colinear requirement of the segment reactions to calculate the x, y position of each successive node point, beginning at point a and progressing to b. If point b fails to fall at the specified support location then the assumed value of $\bar{B}$ is in error. Then a corrective procedure is instituted by the addition of force $\Delta\bar{B}$ to $\bar{B}$ in the direction from b' to b (Figure 2.5-2) to improve upon the previous value. The procedure is repeated until convergence is achieved and point b falls at the prescribed cable support location. When this occurs, a unique solution for the static equilibrium configuration is achieved.

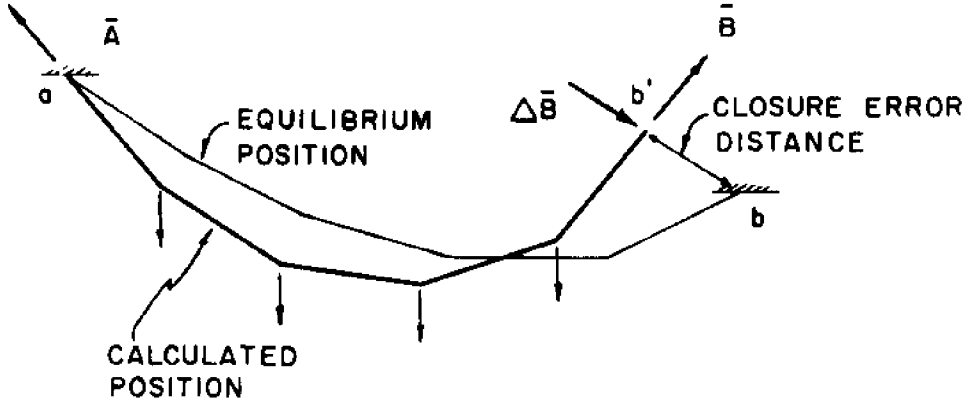

Figure 2.5-2 INTERMEDIATE CABLE POSITION DURING NUMERICAL EQUILIBRIUM CALCULATION

The method will be mathematically formalized in the subsequent section.

2.6. Numerical Procedure and Equations for Statically Analyzing the Two-Point Mooring

The Cartesian coordinate system and notation adopted in this section will correspond to Figure 2.6-1. The coordinate origin is placed at the left anchorage and denoted as the 0^{th} node position. The coordinate system will be oriented relative to the mooring such that the right anchorage, defined as the m^{th} node position, lies on or above the x coordinate axis.

Left anchor node position	$x(0),\ y(0),\ z(0)$
Right anchor node position	$x(m),\ y(m),\ z(m)$

Node point locations will be denoted as the i^{th} position beginning at the left anchor and numbering consecutively to the right anchor or m^{th} station. The external force components acting at the i^{th} node point will be denoted as

$$F_x(i),\ F_y(i),\ F_z(i)\ .$$

The components of the resultant force at the i^{th} node are designated to be

$$R_x(i),\ R_y(i),\ R_z(i)$$

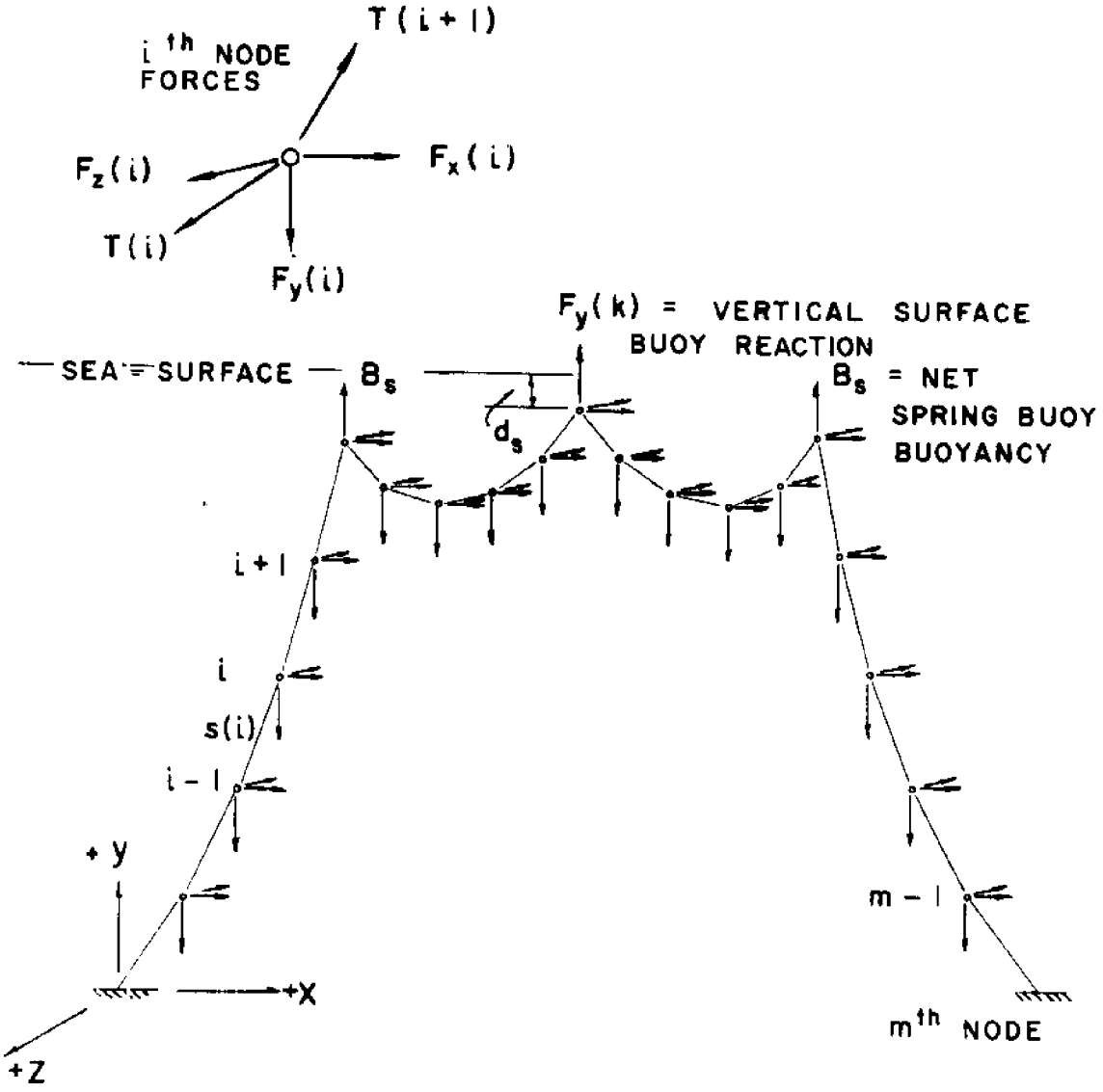

Figure 2.6-1 DISCRETE PARAMETER REPRESENTATION OF TWO-POINT MOORING SYSTEM

The length of the segment immediately preceding the i^{th} node will be denoted as $s(i)$, making the first segment in the cable system $s(1)$. The tension force in the i^{th} segment is $T(i)$. The position of each of the mooring node points are then denoted by the Cartesian coordinates

$$x(i),\ y(i),\ z(i)$$

The components of the resultant force at the i^{th} node are obtained by use of the following equations

$$\begin{aligned} R_x(i) &= F_x(i) + R_x(i+1) \\ R_y(i) &= F_y(i) + R_y(i+1) \\ R_z(i) &= F_z(i) + R_z(i+1) \end{aligned} \qquad (2.6\text{-}1)$$

where $i = 1, 2, \cdots, m-1$. At the last node point $(i=m)$, the resultant force components are given by

$$\begin{aligned} R_x(i) &= R_x(i) \\ R_y(i) &= R_y(i) \\ R_z(i) &= R_z(i) \end{aligned} \qquad (2.6\text{-}2)$$

The tension in the i^{th} segment is determined using

$$T(i) = [(R_x(i))^2 + (R_y(i))^2 + (R_z(i))^2]^{\frac{1}{2}} \qquad (2.6\text{-}3)$$

Successive node point positions are then calculated by the following

relations

$$x(i) = x(i-1) + \frac{R_x(i)s(i)}{T(i)}$$

$$y(i) = y(i-1) + \frac{R_y(i)s(i)}{T(i)} \qquad (2.6\text{-}4)$$

$$z(i) = z(i-1) + \frac{R_z(i)s(i)}{T(i)}$$

Convergence

The two-point mooring in contrast to the cable has three restraining boundary conditions, which the equilibrium configuration must satisfy. These are the fixed left and right anchor positions, and the vertical location of the surface buoy which must be consistent with the displacement characteristics of the buoy, water depth, and the downward reactions created by the mooring. However, there are no restrictions placed on the buoy's horizontal or x-z position.

Where either a buoy or other type of floating object has a relatively large displacement, and therefore will undergo only minor changes, it is possible that the downward displacements (which are small when compared to the systems dimensions) can be safely neglected in analyzing the mooring. However, where vertical displacement is significant, this must be accounted for in applying the closure test at the end of each iteration.

Convergence of the iterative procedure is achieved by successive application of corrective forces at the right anchor surface buoy positions. Corrections are proportional to error and are applied in a direction such that the cable configuration moves to satisfy the restraints imposed on it by the anchor positions and surface buoy. The closure error at the right anchor position is calculated by

$$E_m = (x_m - x(m))^2 + (y_m - y(m))^2 + (z_m - z(m))^2 \qquad (2.6\text{-}5)$$

where x_m, y_m, z_m are the coordinates of the fixed right anchor. The surface buoy closure error is given by

$$E_b = ((D - d_s) - y(k))^2 \qquad (2.6\text{-}6)$$

where k denotes the surface buoy index. Consequently the total closure error can be defined to be

$$E = E_m + E_b \qquad (2.6\text{-}7)$$

This equation contains the sum of the squares of the closure error distances. Corrective anchor reaction forces are obtained by use of

$$\Delta_x = \frac{\delta}{\sqrt{E}} (x_m - x(m))$$

$$\Delta_y = \frac{\delta}{\sqrt{E}} (y_m - y(m)) \qquad (2.6\text{-}8)$$

$$\Delta_z = \frac{\delta}{\sqrt{E}} (z_m - z(m))$$

The corrective force at the buoy position is given by

$$\Delta_b = \frac{\delta}{\sqrt{E}} ((D - d_s) - y(k)) \qquad (2.6\text{-}9)$$

δ is a positive value which is initially chosen, then selectively reduced so that each successive iteration produces a successively smaller closure error, until the value of E is less than some preselected value K. An improved set of reaction values is then obtained by adding the corrective values to the previous set of reactions. Interval halving was selected for the systematic reduction of δ. The procedure is flow charted in the next section. At each iteration the value of the total error E is tested to see whether it is less than that of the previous iteration. If it is, then a successful iteration has been performed and the current value of δ is retained until E is found to be larger than that of the preceding E. At this point in the solution, the program neglects the current set of iteration values, δ is reduced and the solution proceeds from the last stored iteration set. A new set of values is then calculated, E is again tested and either retained or further reduced accordingly.

Figure 2.6-2 is presented to illustrate the three dimensional convergence of the procedure as the configuration progresses towards its equilibrium position from intentionally selected, poor initial values of both the reactions and convergence factor δ. Table 2.6-1 gives the calculated reactions and closure values at selected iterations.

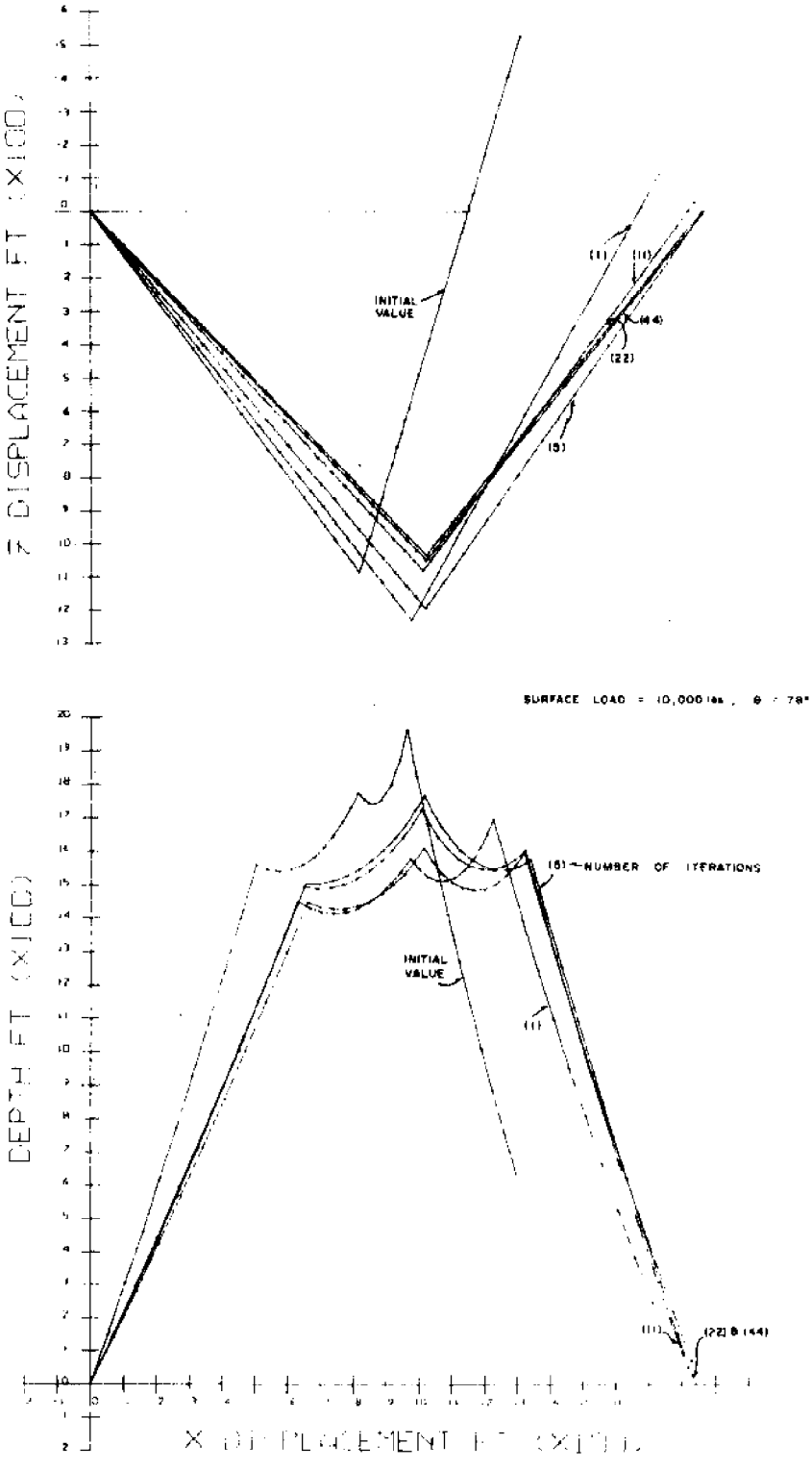

Figure 2.6-2 MOORING GEOMETRY AT SUCCESSIVE ITERATIONS

Table 2.6-1. Convergence Example of the Two-Point Mooring To A Static Equilibrium Configuration

Iteration	Vertical Surface Buoy Reaction	Left Anchor Reactions			Rt. Anchor Reactions						
		$R_x(0)$	$R_y(0)$	$R_z(0)$	$R_x(m)$	$R_y(m)$	$R_z(m)$	E_b	E_m	E	δ
Initial values	10000.00	-	-	-	1500.00	-5000.00	-5000.00	63.17	977058.92	977122.09	1500.0
1	9987.94	-4405.34	-9182.16	-5578.27	2326.23	-5965.57	-4203.21	35237.57	88366.35	123603.92	1500.0
2	10788.84	-4950.70	-8940.09	-6050.87	2871.58	-7008.55	-3730.61	73850.43	28913.50	102763.93	1500.0
5	12032.24	-4884.80	-9767.58	-5752.36	2805.68	-7424.46	-4029.12	24882.80	5744.85	30627.35	750.0
7	13312.45	-5066.49	-10320.57	-5717.50	2987.37	-8151.68	-4063.98	11626.23	2110.26	13736.50	750.0
11	14539.96	-5177.43	-10975.11	-5560.91	3098.32	-8724.65	-4220.57	1750.95	3481.26	5232.21	375.0
15	15062.54	-5298.46	-11140.91	-5611.32	3219.34	-9081.43	-4170.15	1291.56	286.96	1578.52	187.5
22	15739.57	-5408.23	-11437.64	-5590.49	3329.11	-9461.74	-4190.98	205.89	69.38	275.27	93.75
30	15956.53	-5435.27	-11547.92	-5566.28	3356.15	-9568.41	-4215.20	24.74	5.08	29.83	23.44
40	16073.93	-5451.58	-11605.08	-5555.76	3372.46	-9628.65	-4225.72	0.16	4.55	4.72	11.72
44	16082.17	-5455.13	-11604.85	-5559.81	3376.01	-9637.11	-4221.67	0.69	0.27	0.97	5.86

Run Information:

Surface Loading = 10,000 lbs $\theta = 78.0^{\circ}$, $\kappa = 1.0$

D = 1800.0 ft., x_m = 1840.0 ft., B_s = 14,000 lbs L_a = 1770.0 ft

L_c = 600.0 ft., d_s = 32.0 ft. No. of nodes = 40

2.7. Computer Program for Static Mooring Response

A flow chart showing the calculation procedure employed, based upon the equations presented in Section 2.6 is presented in Figure 2.7-1. The subroutines called from the main program will be briefly discussed with reference to their purpose and usage.

Subroutine DEADLD

This subroutine, furnished with the weight and length of the mooring cables, spring buoy buoyancy and the stipulated number of node points in each cable, breaks down the distributed loading into an equivalent discrete system of vertical forces. Interior node forces account for the weight of a full segment, where those at the anchor ends equal 1.5 that of an interior node to account for the total cable weight.

Subroutine DISPLACE

Subroutine DISPLACE provides for vertical displacement of the buoy or other object located at the surface termination point of the mooring. This routine is written for a specific object geometry, such that vertical mooring reactions on it can be correlated with consequential changes in its displacement. The subroutine is fitted into the basic iteration procedure for calculating the equilibrium position

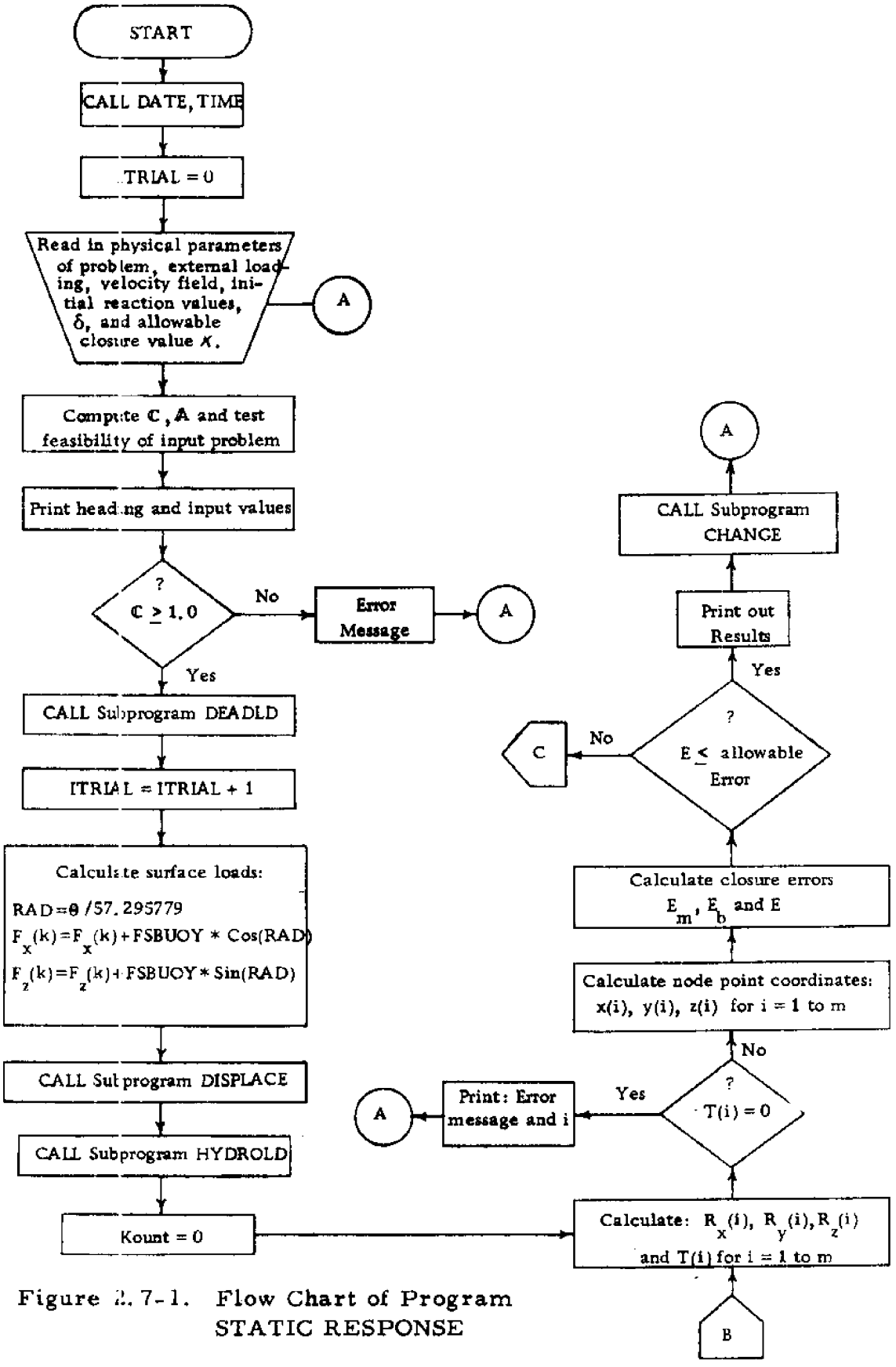

Figure 2.7-1. Flow Chart of Program STATIC RESPONSE

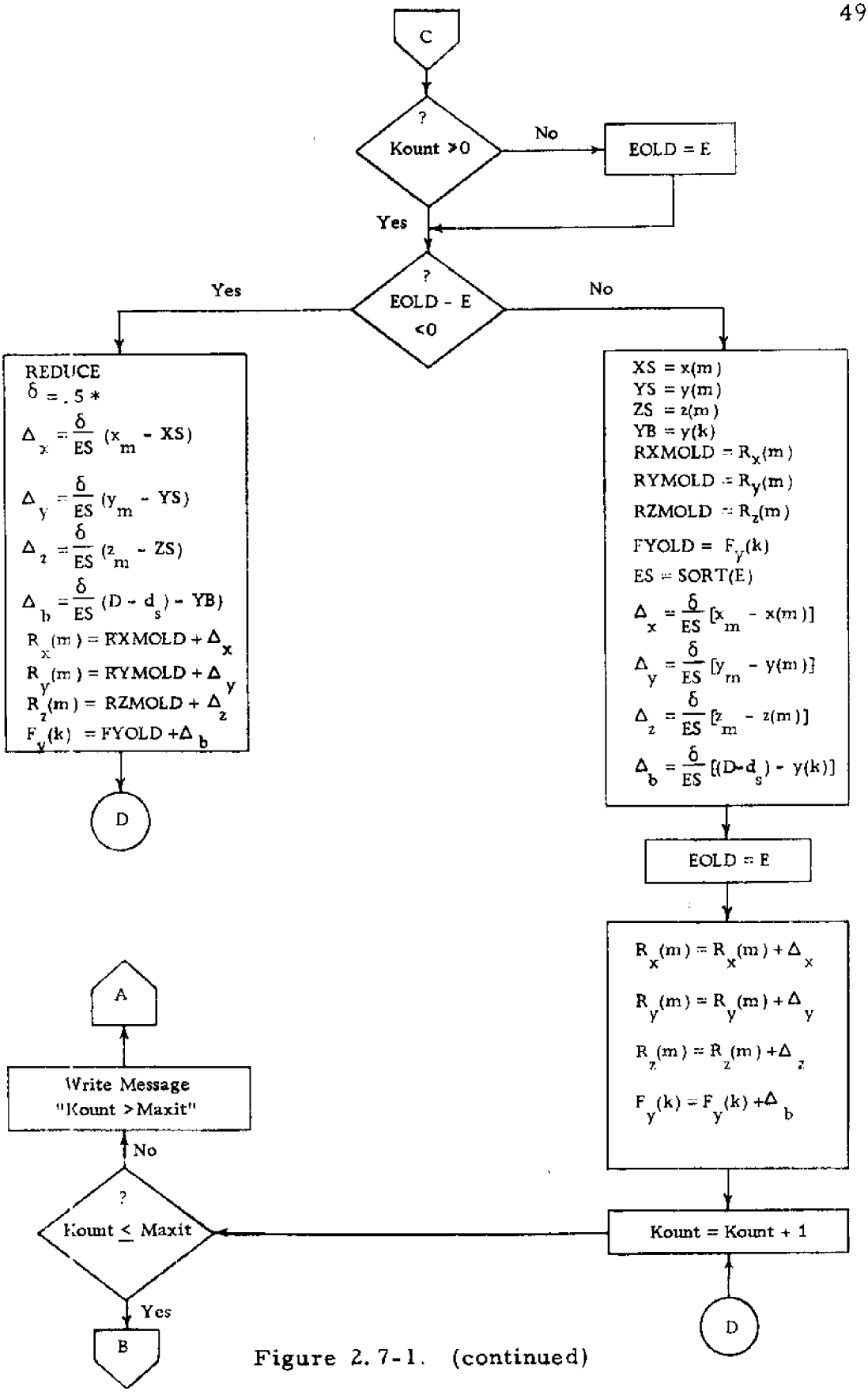

Figure 2.7-1. (continued)

with the additional constraint that vertical displacement be compatible with the vertical reaction on the object.

Subroutine HYDROLD

This subroutine calculates the hydrodynamic drag on all cable elements produced by subsurface currents. The program is written to account for any number of horizontal velocity fields of arbitrary magnitude, depth and direction. Hydrodynamic forces are evaluated by means of the drag equation applied to a cylindrical cable element. More complex loading functions are possible and can be easily incorporated in the program if desired. Required inputs to the subprograms are the velocity field specification, the physical and hydrodynamic properties of each of the component cables of the mooring. Subsurface drag on the spring buoys is accounted for through use of subprogram CHANGE.

The projected length of each of the cable elements, perpendicular to the velocity field $\bar{v}$, is obtained by

$$s^p(i) = \left(s^2(i) - \left(\bar{s}(i) \cdot \frac{\bar{v}}{|\bar{v}|}\right)^2\right)^{\frac{1}{2}} \qquad (2.7\text{-}1)$$

which, when expanded gives

$$s^p(i) = \left[\left(s(i)_x^2 + s(i)_y^2 + s(i)_z^2\right) - \left(\frac{s(i)_x v_x + s(i)_z v_z}{|\bar{v}|}\right)^2 \right]^{\frac{1}{2}} \qquad (2.7-2)$$

As shown in Figure 2.7-2 $s^p(i)$ is the component length of $s(i)$ perpendicular to the velocity field

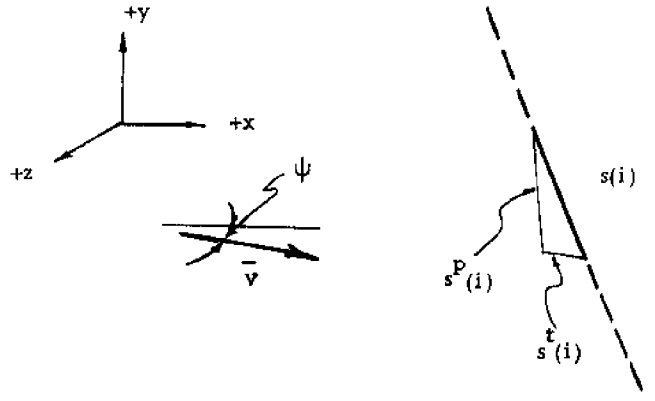

Figure 2.7-2. Cable Element Oriented in a Velocity Field

The total hydrodynamic force $Fd(i)$ acting on the i^{th} cable element is calculated by means of

$$Fd(i) = \tfrac{1}{2} \rho C_d d\, s^p(i) |v| v \qquad (2.7-3)$$

where ρ = mass density of the fluid

C_d = drag coefficient

d = cable diameter

$Fd(i)$ is reduced to component form by means of

$$Fd_x(i) = Fd(i) \cos \psi$$
$$Fd_z(i) = Fd(i) \sin \psi \qquad (2.7-4)$$

The total component force is then subdivided and distributed equally to each adjacent node.

Subroutine CHANGE

This subroutine allows for multiple calculation of several successive mooring configurations with different loadings. It also provides the means for changing one or more parameters of the problem. This provides for improved economical solutions. For example, in successively changing the external forces applied to the system, the previous reaction values etc. are retained and used as initial guesses to the next problem. The program also provides the capability for changing the structural or hydrodynamic characteristics of given elements of a mooring after the application of subroutine DEADLD. This provides the means for altering the basic system to a more intricate or totally new one.

2.8. Evaluation of the Numerical Method

Although Skop and O'Hara indicated that increased accuracy would be achieved with the usage of a larger number of cable segments, no indication as to the accuracy of the method was presented. The question of errors of unknown extent, due to the inexact treatment of the cable weight, was raised by O'Brien but left unanswered relative to the string polygon formulation analysis procedure

proposed by Michalos and Birnstiel (1962).

In order to ascertain the accuracy to be expected from a discrete parameter formulation and to provide guidance in selecting the number of cable segments necessary, two criteria were set up.

Program CABLE was developed for statically analyzing a single cable, utilizing the same numerical method adopted for the two-point mooring analysis. Solutions were obtained and compared to those of the continuum case provided by program CATENARY. Three cable geometries of equal length and weight but differing in support positions were investigated.

Case	$\frac{x_t}{L}$	$\frac{h}{x_t}$
I	.80	0
II	.60	0.832
III	.40	2.180

Solutions to each of the three cases were obtained with a varying number of cable segments. In each case K was taken as 0.01. Comparison of the relative tension for each of the three cases as a function of the number of segments is shown in Figure 2.8-1. In order to give added quantitative interpretation to these results, the same data is presented in Figure 2.8-2 plotted as percent deviation from the exact solution. It is of interest that in Case II the tension values at the lower or left reaction are nearly exact for as few as

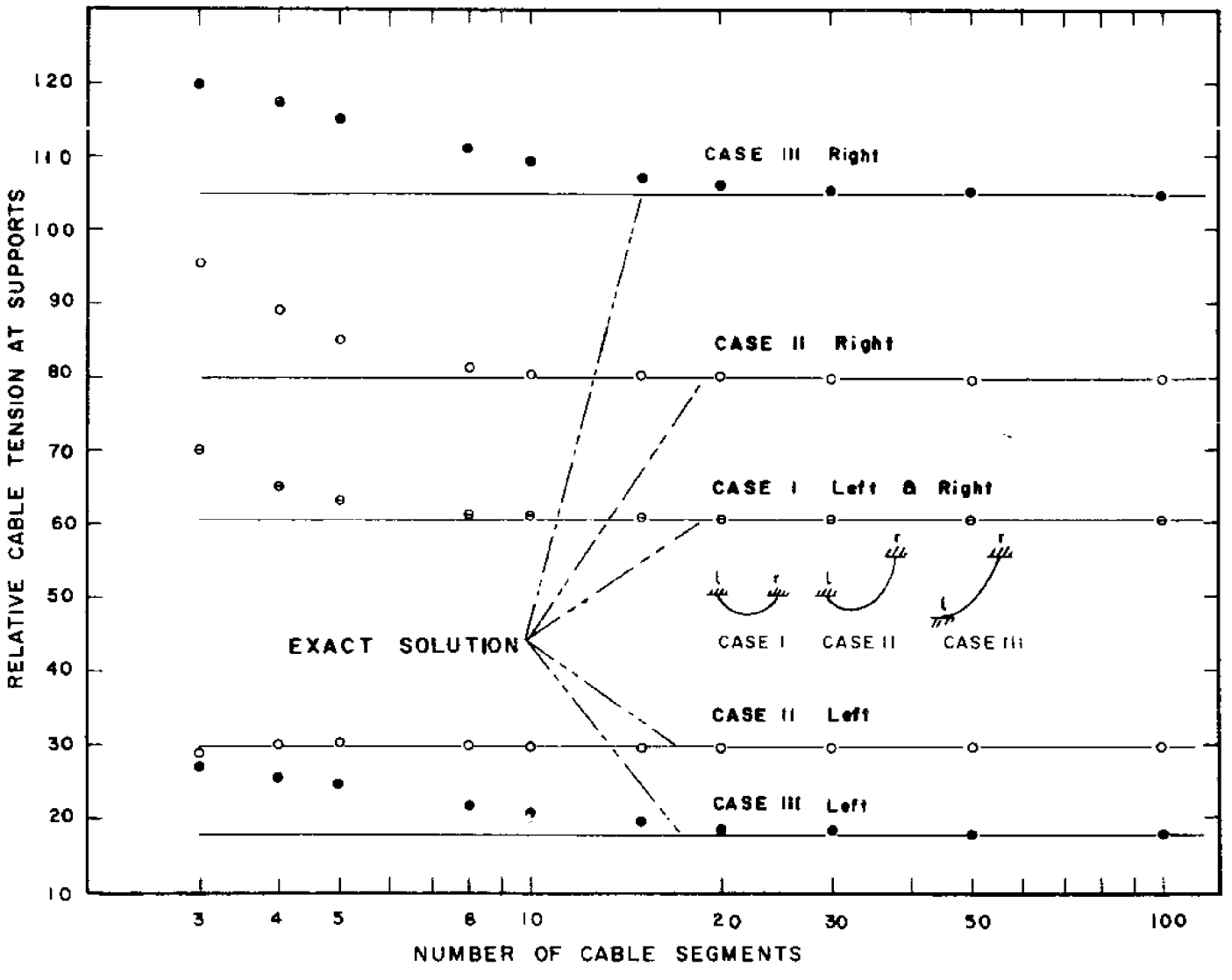

Figure 2.8-1 COMPARISON OF THE DISCRETE & CONTINUUM CABLE SOLUTIONS

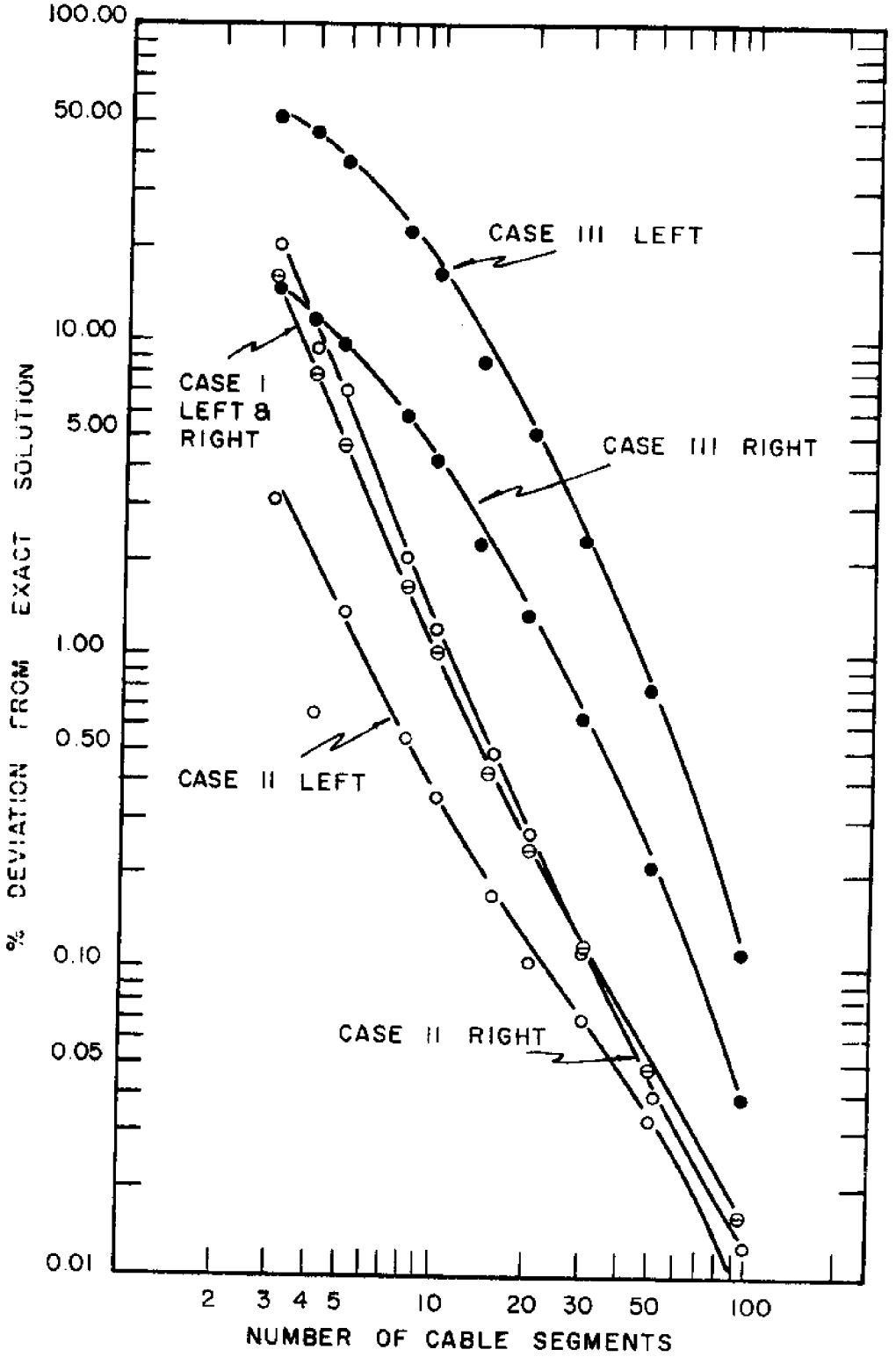

Figure 2.8-2 PERCENT DEVIATION OF DISCRETE SOLUTION FROM EXACT SOLUTION

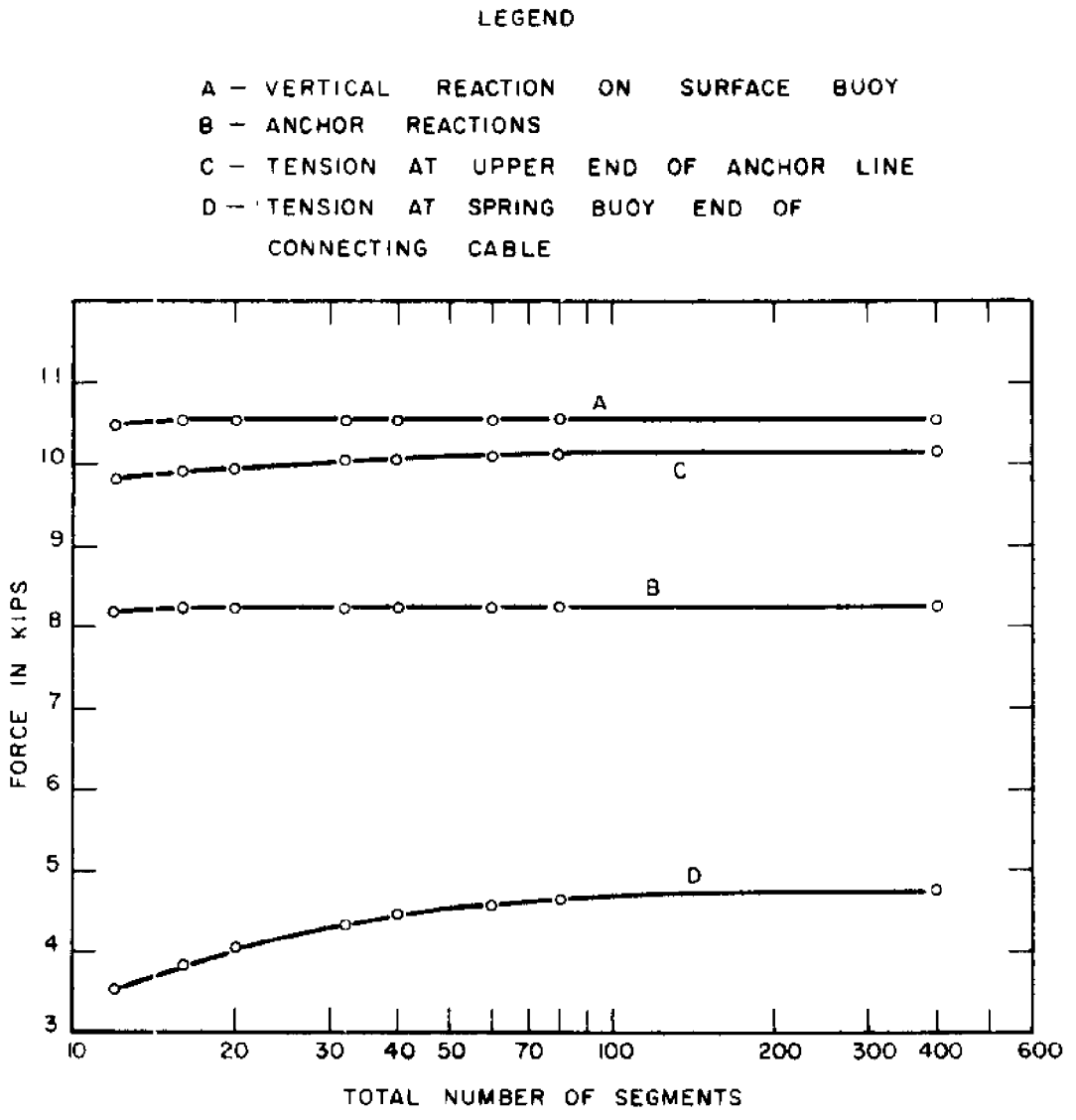

Figure 2.8-3 TWO – POINT MOORING REACTIONS VS NUMBER OF CABLE SEGMENTS

three segments, whereas in Case III the tension values at the left reaction are the most divergent of the cases considered. The right reaction values of Case III also exhibit this same behavior but to a lesser degree.

In order to view the combined effect that the number of segments in a connected array of cables has, a two-point mooring configuration (Table 2.9-1) was varied using an equal number of segments in each of the component cables, and then compared to itself. A quasi-exact solution might be considered as that case where variation in the results is non-discernible. A minimum number of 12 segments to a maximum of 400 were used. The effect of this variation on the cable tension at selected points and on the moorings' reactions is shown in Figure 2.8-3.

2.9. Parameter Investigation

Because infinite possibilities exist for component combinations and hence mooring configurations, a systematic method of describing a particular system is desirable. In discussing the mooring, all configurations will be referenced to their static equilibrium position in the absence of externally applied loads. To provide descriptive aid, the following dimensionless parameters are introduced and illustrated in Figure 2.9-1. The aspect ratio is defined by

$$\mathbf{A} = \frac{D - d_s}{x_m} \qquad (2.9\text{-}1)$$

The ratio of the anchor line length to that of the buoy connecting cable will be defined as

$$\mathbb{L} = \frac{L_a}{L_c} \qquad (2.9\text{-}2)$$

The compliancy number, which is a quantifier of the yielding capacity of the mooring has a minimum value of 1, and is defined by

$$\mathbb{C} = \frac{L_a + L_c}{\sqrt{(D-d_s)^2 + (\frac{x_m}{2})^2}} \qquad (2.9\text{-}3)$$

The spread ratio defined as the horizontal distance between spring buoy positions divided by the anchor span, is

$$\mathbb{S} = \frac{2x_t}{x_m} \qquad (2.9\text{-}4)$$

In order to isolate and determine the relative effect that the basic components of the two-point mooring play in its static behavior, a parameter study based on the independent variation of selected components was undertaken. Use of the numerical computer program was made to perform the necessary calculations.

Due to the infinite combination of components it was impractical to investigate a very wide range of possible configurations. Consequently a standard reference configuration similar to the deployed

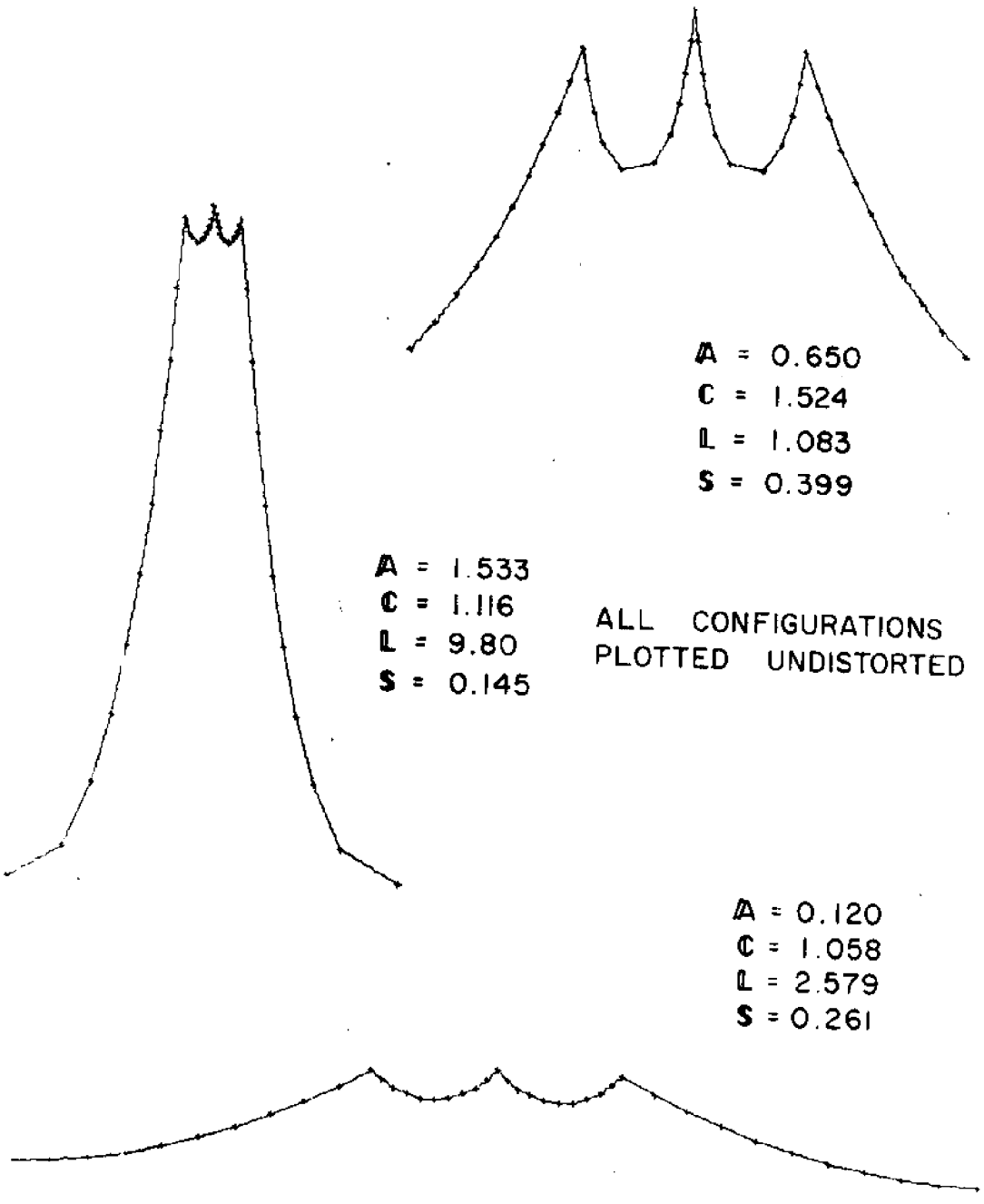

Figure 2.9 - 1 COMPARISON OF DIMENSIONLESS PARAMETERS WITH MOORING GEOMETRY

prototype system was adopted and a parametric study based on variation about this configuration was conducted. The reference configuration is given in Table 2.9-1. The parameters selected for variation were: the spring buoy buoyancy, depth of water accompanied by a proportional change in anchor line length, location of the connecting chain position on the surface buoy, anchor span, and weight of the buoy connecting chain and anchor lines. Figures 2.9-2 through 2.9-13 show the effect that variation of each of these parameters has on the mooring reactions and on cable tensions at selected points, as well as accompanying geometry changes of the mooring. All figures were developed using a total of 60 node points, 10 in each of the buoy connecting cables and 20 in the anchor lines. An error of closure was taken to be less than or equal to 0.10. It was felt that this combination represented a good compromise between necessary accuracy and computer time expenditure. Adaption of these requirements was based on the evaluation presented in Section 2.8. It is noteworthy that each of the parameters exhibits a near linear effect over at least some portion of the selected range of variations. Figure 2.9-9 shows that increasing the anchor span and consequently decreasing the compliancy number of the system has the effect of increasing all of the internal and external reactions of the system. A mooring design for a particular site and condition would entail establishing the proper combination of components to optimize the

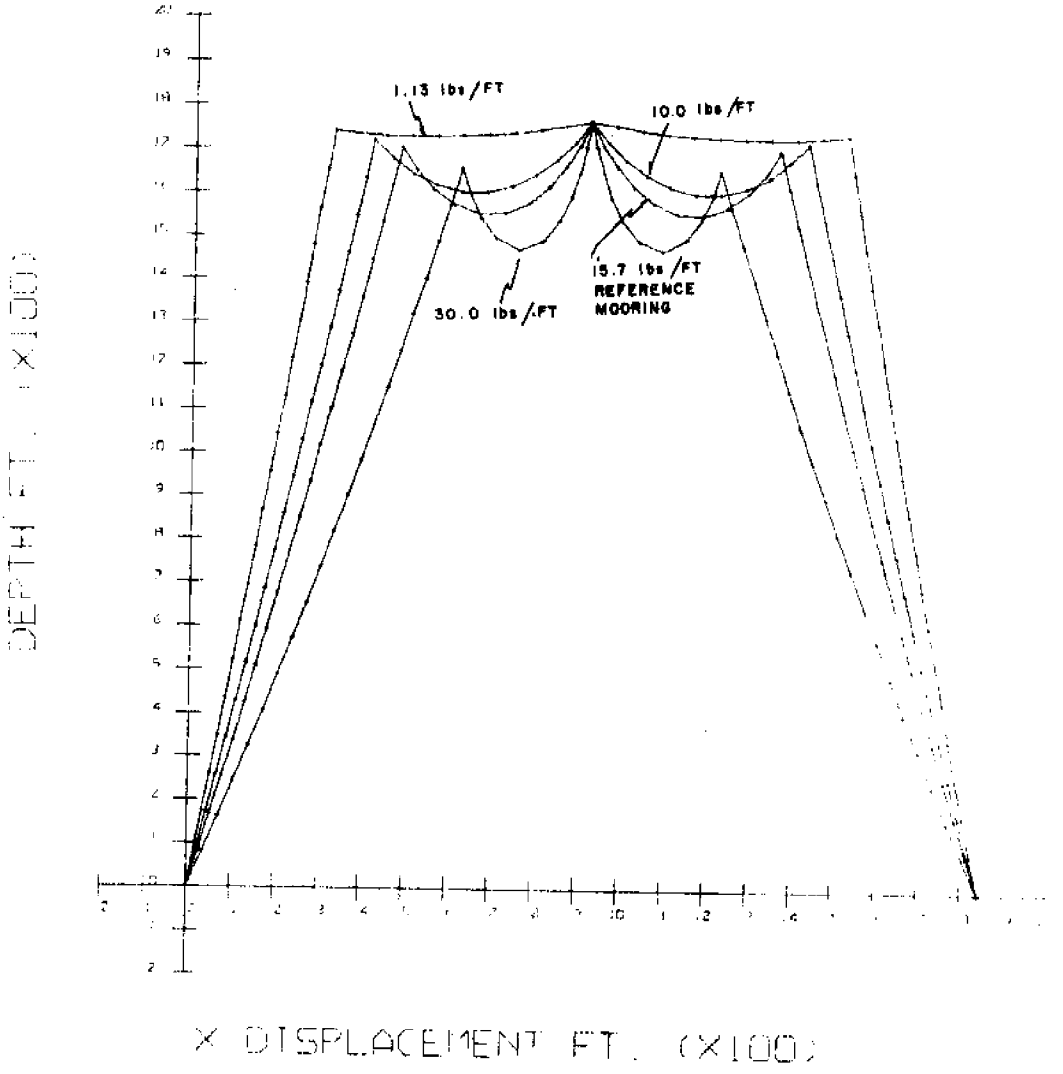

Figure 2.9-2 MOORING GEOMETRY, RELATED TO CHANGES IN BUOY CONNECTING CABLE WEIGHT

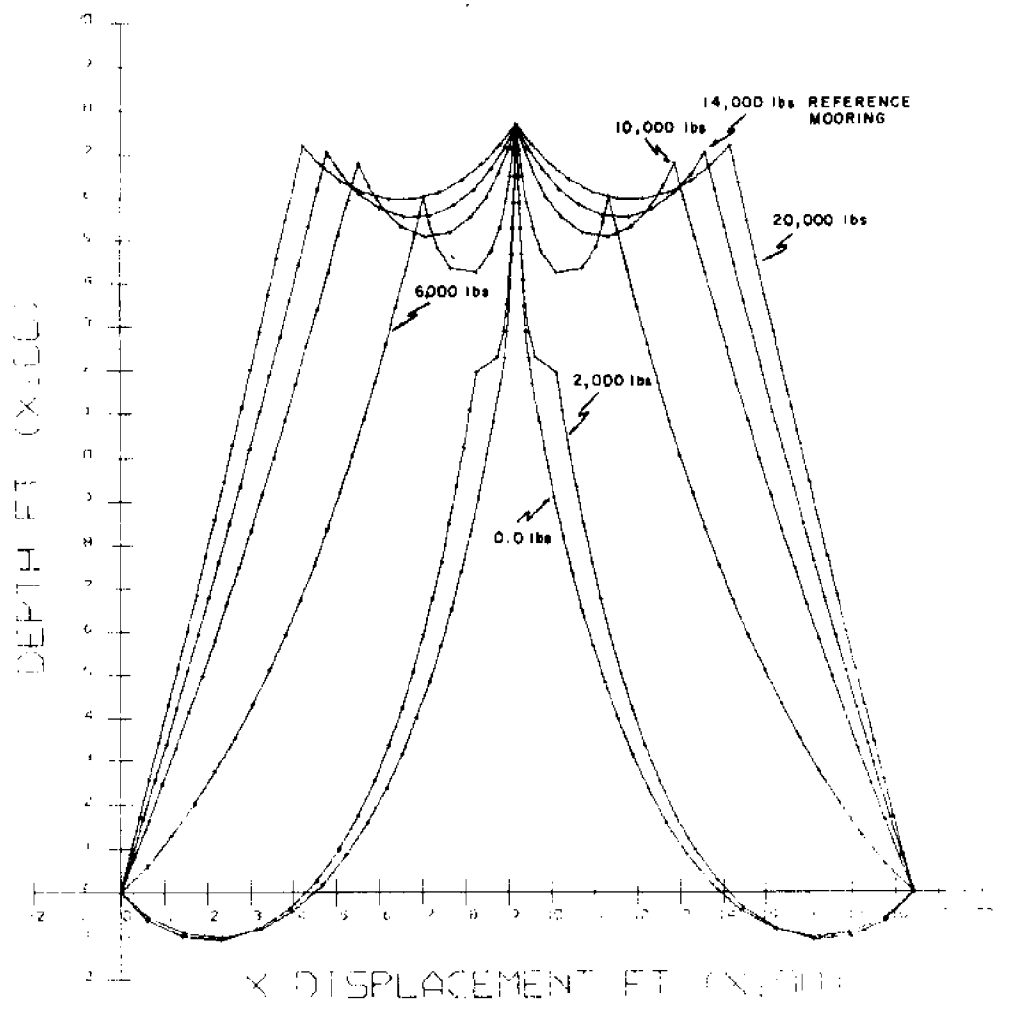

Figure 2.9-3 MOORING GEOMETRY, RELATED TO CHANGES IN SPRING BUOY BUOYANCY

LEGEND

A – VERTICAL REACTION ON SURFACE BUOY
B – ANCHOR REACTIONS
C – TENSION AT UPPER END OF ANCHOR LINE
D – TENSION AT SPRING BUOY END OF CONNECTING CABLE

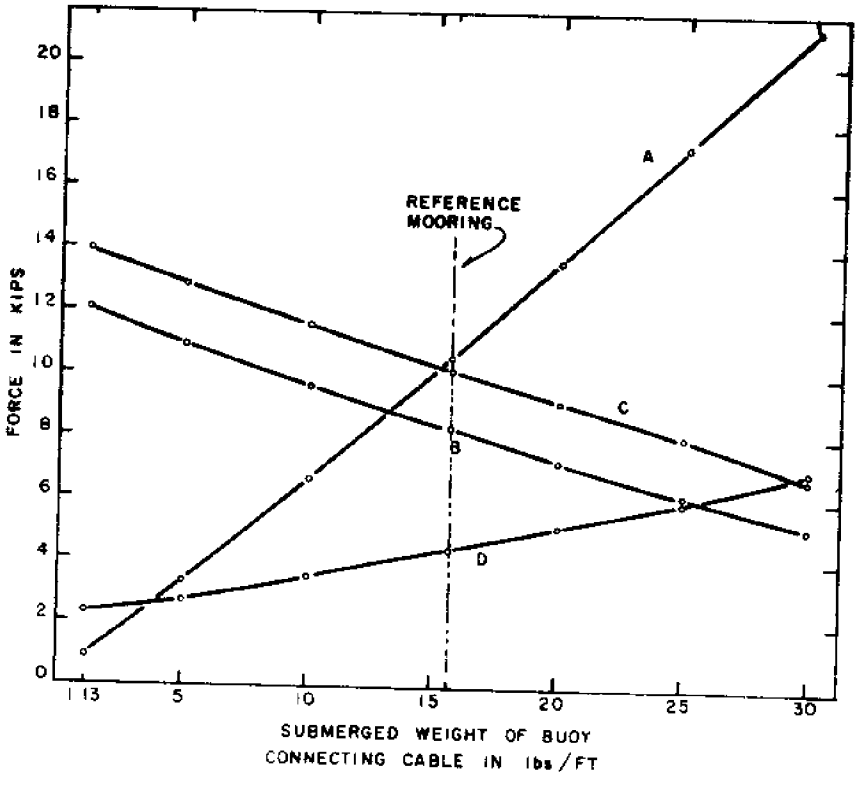

Figure 2.9-4 VARIATION OF BUOY CONNECTING CABLE WEIGHT

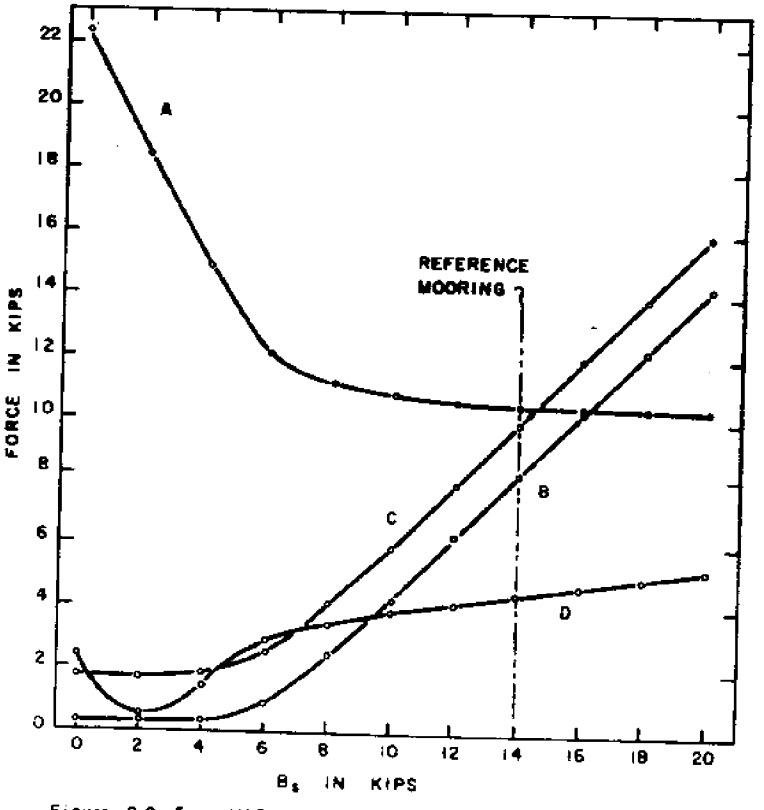

Figure 2.9-5 VARIATION OF NET SPRING BUOY BUOYANCY

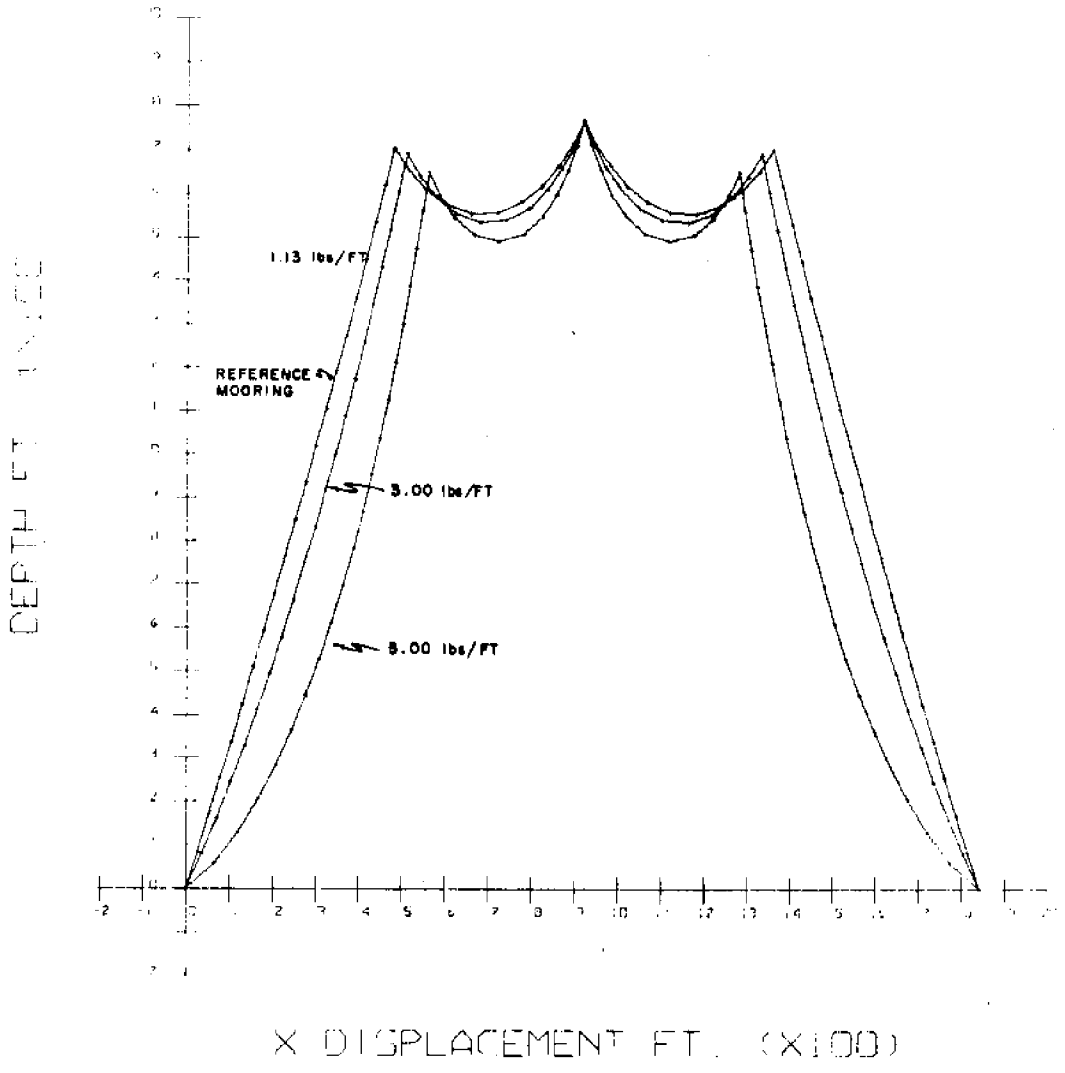

Figure 2.9-6 MOORING GEOMETRY, RELATED TO CHANGES IN ANCHOR CABLE WEIGHT

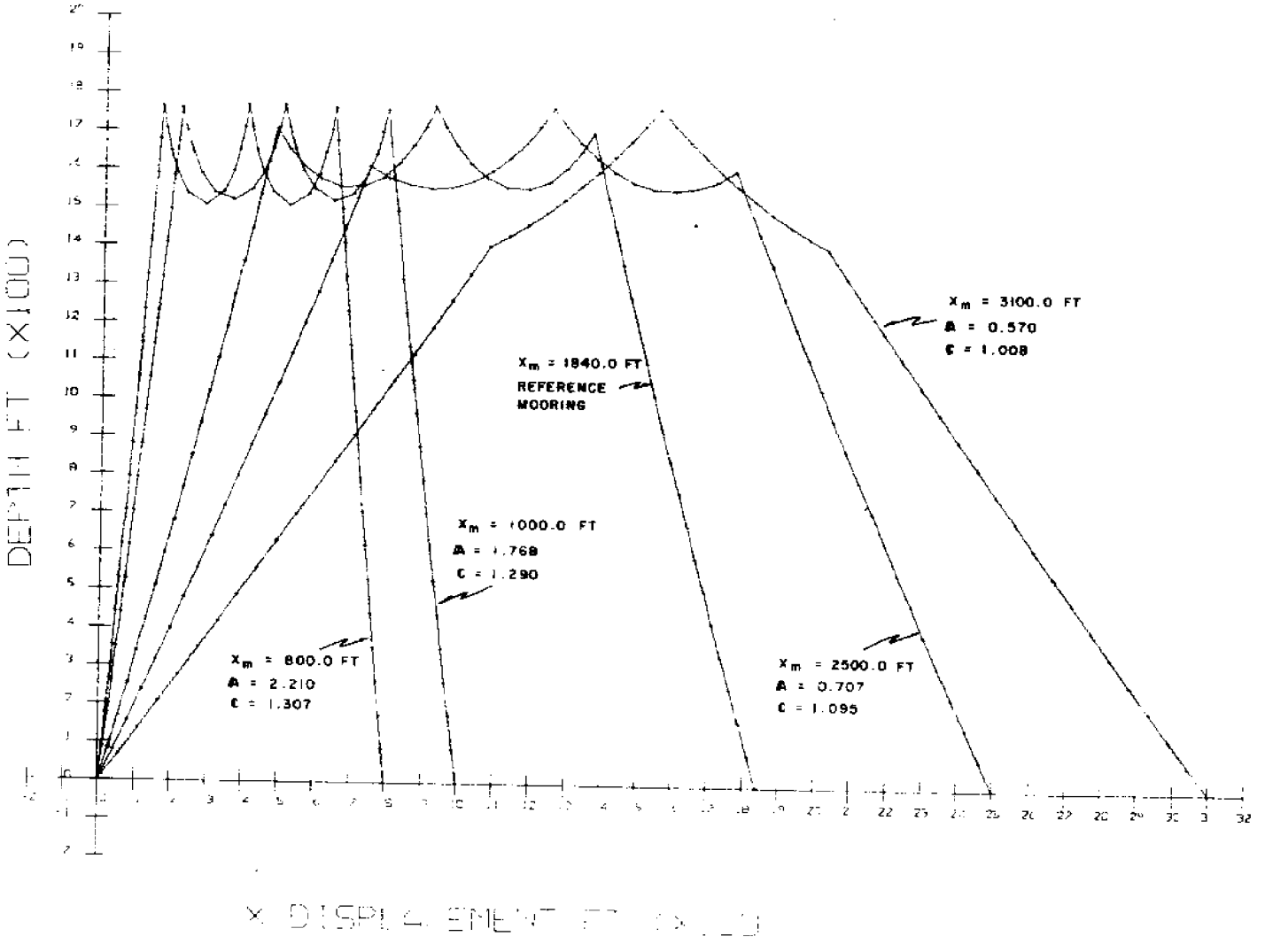

Figure 2.9-7 MOORING GEOMETRY, RELATED TO CHANGES IN ANCHOR SPAN

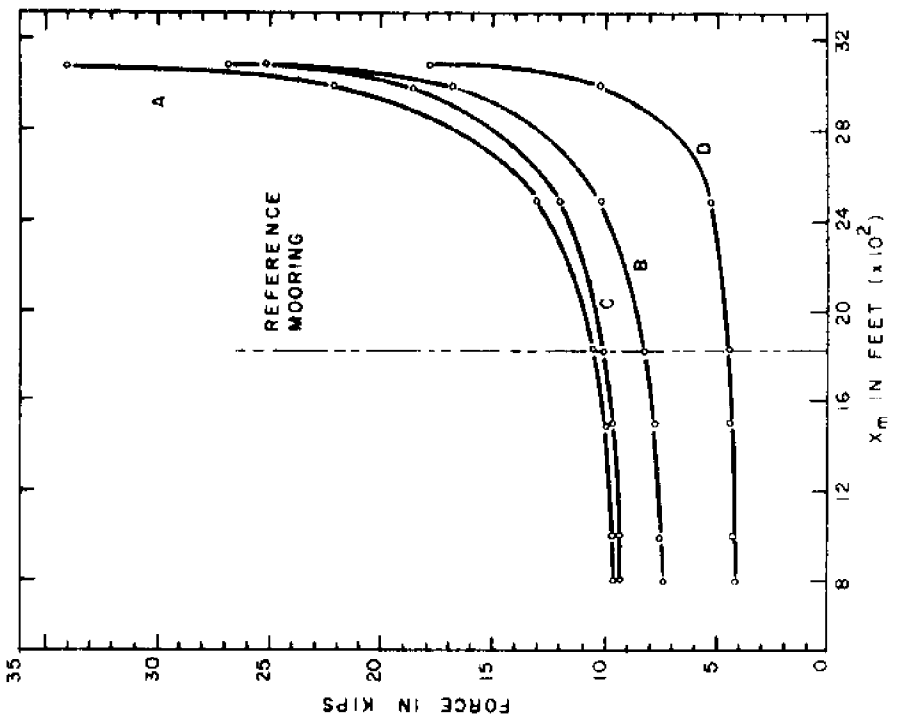

Figure 29-9 VARIATION IN ANCHOR SPAN

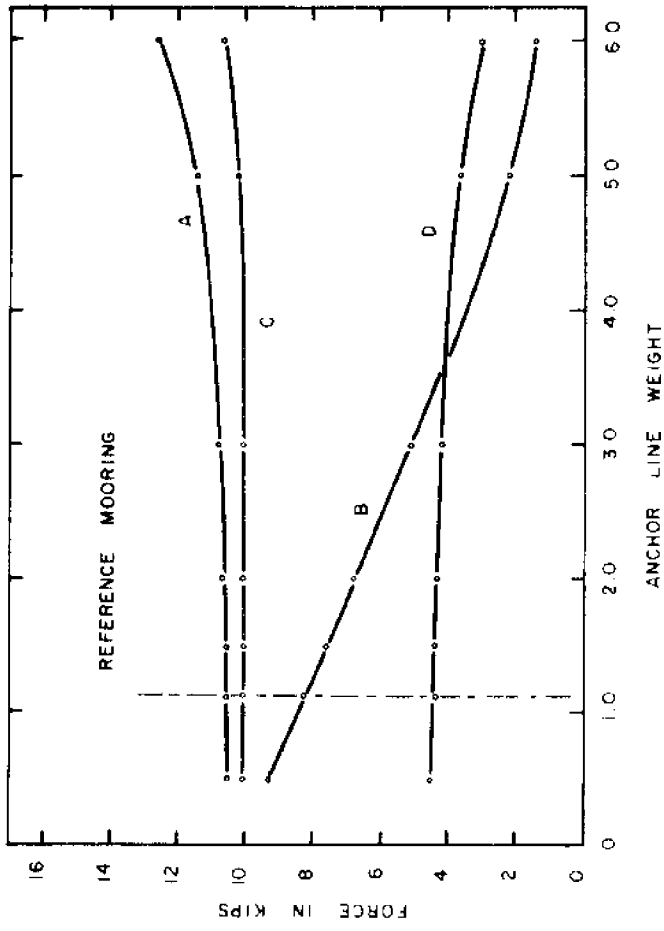

Figure 29-8 VARIATION OF ANCHOR LINE WEIGHT

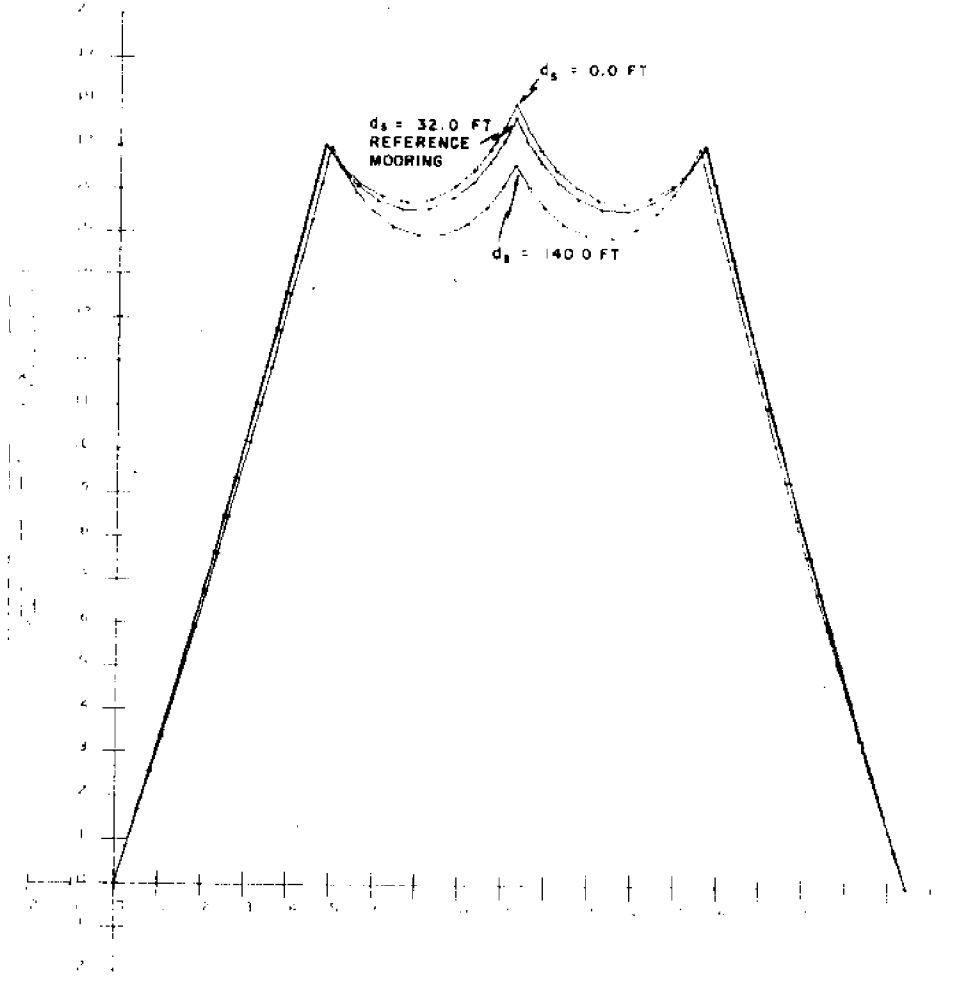

Figure 2.9-10 MOORING GEOMETRY, RELATED TO CHANGES IN BUOY CONNECTING CABLE ATTACHMENT LOCATION

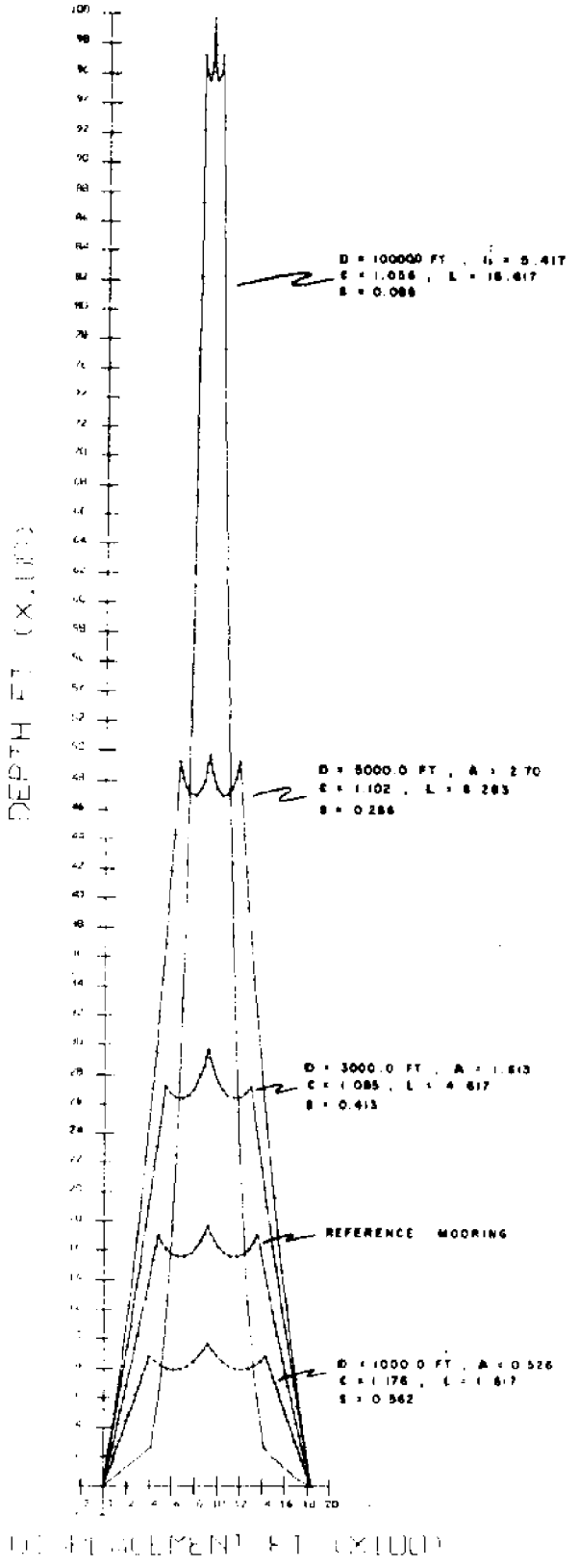

Figure 2.9-11 MOORING GEOMETRY, RELATED TO CHANGES IN DEPTH

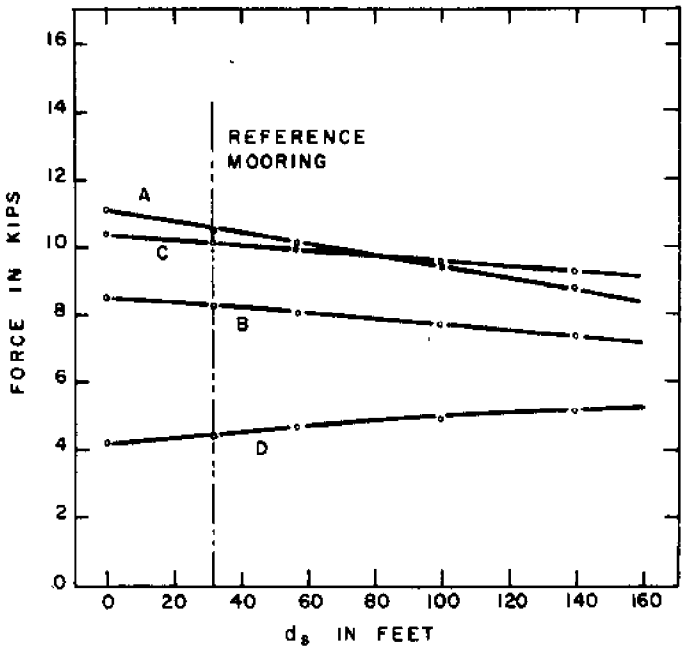

Figure 2.9-12 VARIATION OF THE LOCATION OF BUOY CONNECTING CABLE ATTACHMENT POINT

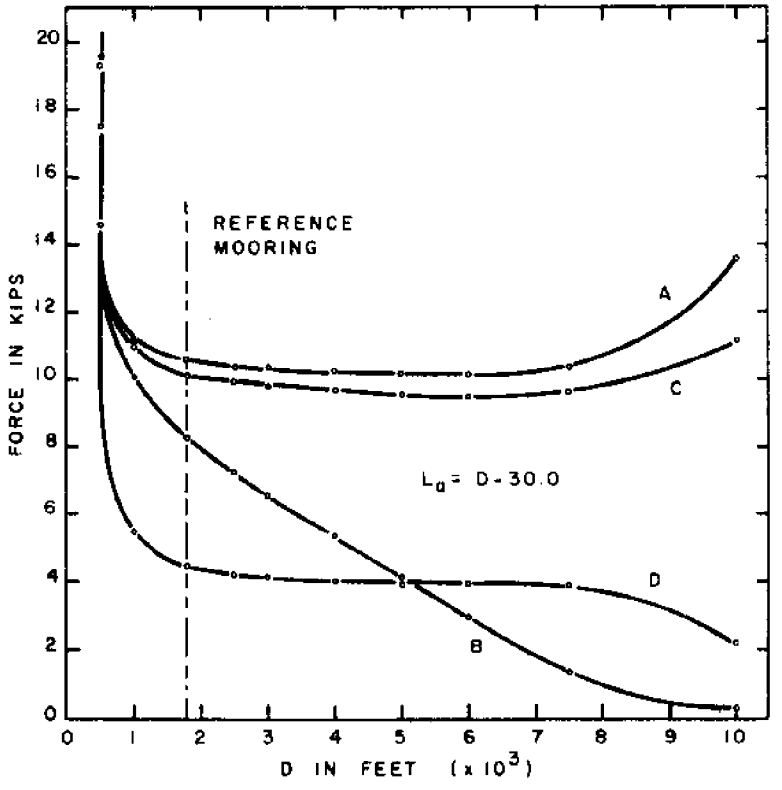

Figure 2.9-13 VARIATION OF DEPTH & ANCHOR LINE LENGTH

system in terms of the applicable gauging criteria.

Table 2 9-1. Reference Configuration Used in the Parameter Study of the Two-point Mooring

Dimensions	Dimensionless Parameters
D = 1800.00 ft.	$\mathbb{A}$ = 0.961
x_m = 1840.00 ft.	$\mathbb{C}$ = 1.189
B_s = 14000 lbs. (net)	$\mathbb{L}$ = 2.950
L_a = 1.13 lbs/ft. (submerged wt.)	$\mathbb{S}$ = 0.479
L_c = 15.70 lbs/ft. (submerged wt.)	
d_s = 32.0 ft.	

2.10. Multi-Directional Loading Effects

The two-point reference mooring was analyzed with respect to surface loads of differing magnitude and direction. The effect of directional loading on the anchor reactions is illustrated by Figure 2.10-1.

Geometric changes produced by each of three different surface loadings are shown in Figures 2.10-2 through 2.10-5, demonstrating the highly compliant nature of the system.

Important to design is a knowledge of the systems maximum horizontal displacement at the surface as well as the internal reaction distribution. Spring buoys must be designed to withstand

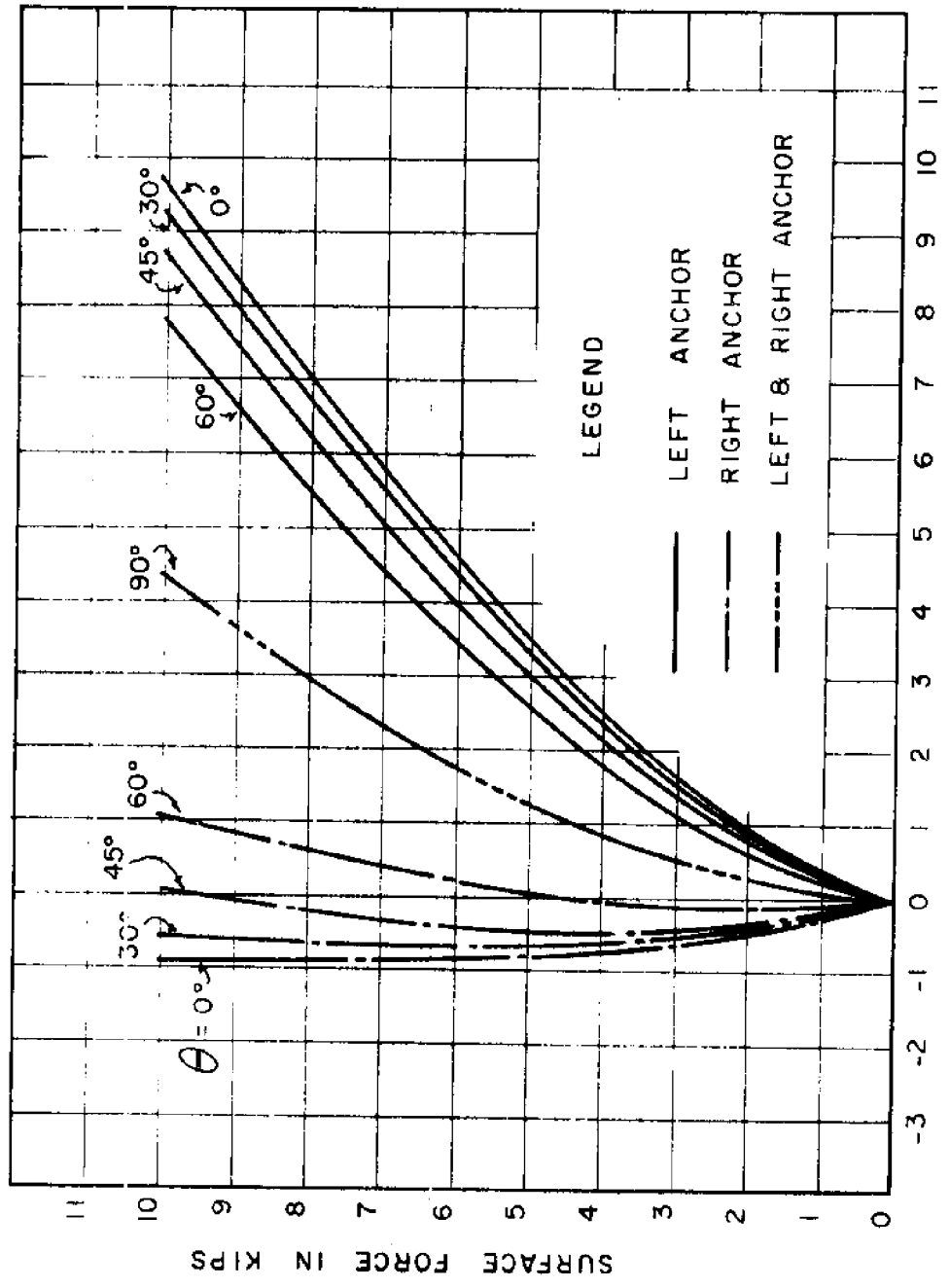

Figure 2.10-1 CHANGE IN ANCHOR REACTIONS FOR REFERENCE MOORING

pressures due to changes in depth that they will be subject to

To demonstrate the effect of hydrodynamic forces on the mooring, an example is considered. A uniform 1 knot velocity field extending throughout the full depth of water is selected and evaluated with respect to its influence on the reference mooring coupled to the TOTEM and spring buoys shown in Figure 1.2-1. Hydrodynamic drag coefficients were derived from Reynolds Number criteria. The coefficients were derived from Reynolds Number criteria. The coefficient used for the buoys was 0.5. This results in a force of 925.0 lbs. at the surface buoy position and a force of 98.5 lbs. at each of the subsurface spring buoy locations. The effective diameters of the anchor line and buoy connecting cables were taken to be 7/8 inch and 1.25 inches, respectively. Cable coefficients used were evaulated as 1.6. The mooring in its initial and displaced position is shown in Figure 2.10-6. The lighter anchor lines exhibit the most pronounced curvature which can most easily be seen in the plan view of the mooring. Reaction changes instituted by the velocity field are observable in the following table.

Reactions	Zero Velocity Field	1 Knot Velocity Field $\psi = 30^{\circ}$
Surface Buoy (Vertical)	10552.70 lbs.	10801.16 lbs.
Left Anchor	8244.35 lbs.	9178.88 lbs.
Right Anchor	8244.35 lbs.	7762.83 lbs.

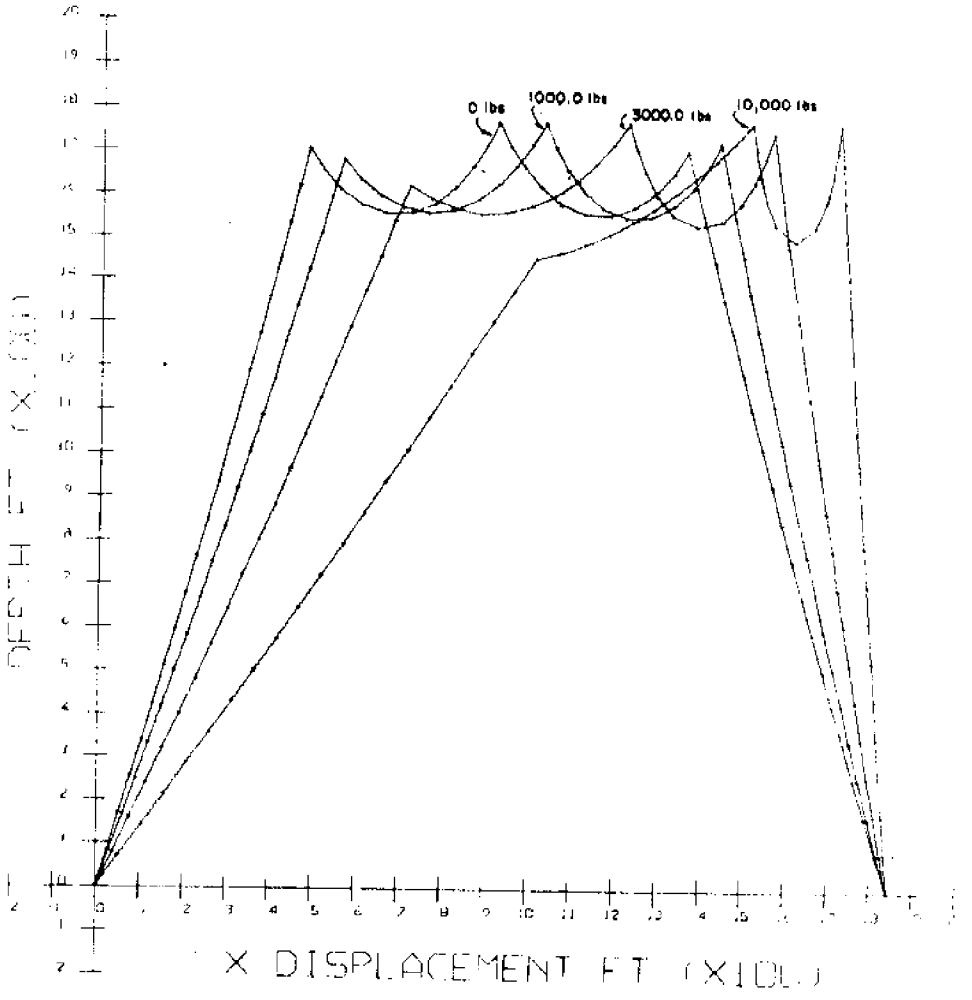

Figure 2.10-2 MOORING GEOMETRY FOR SURFACE LOADS AT $\theta = 0°$

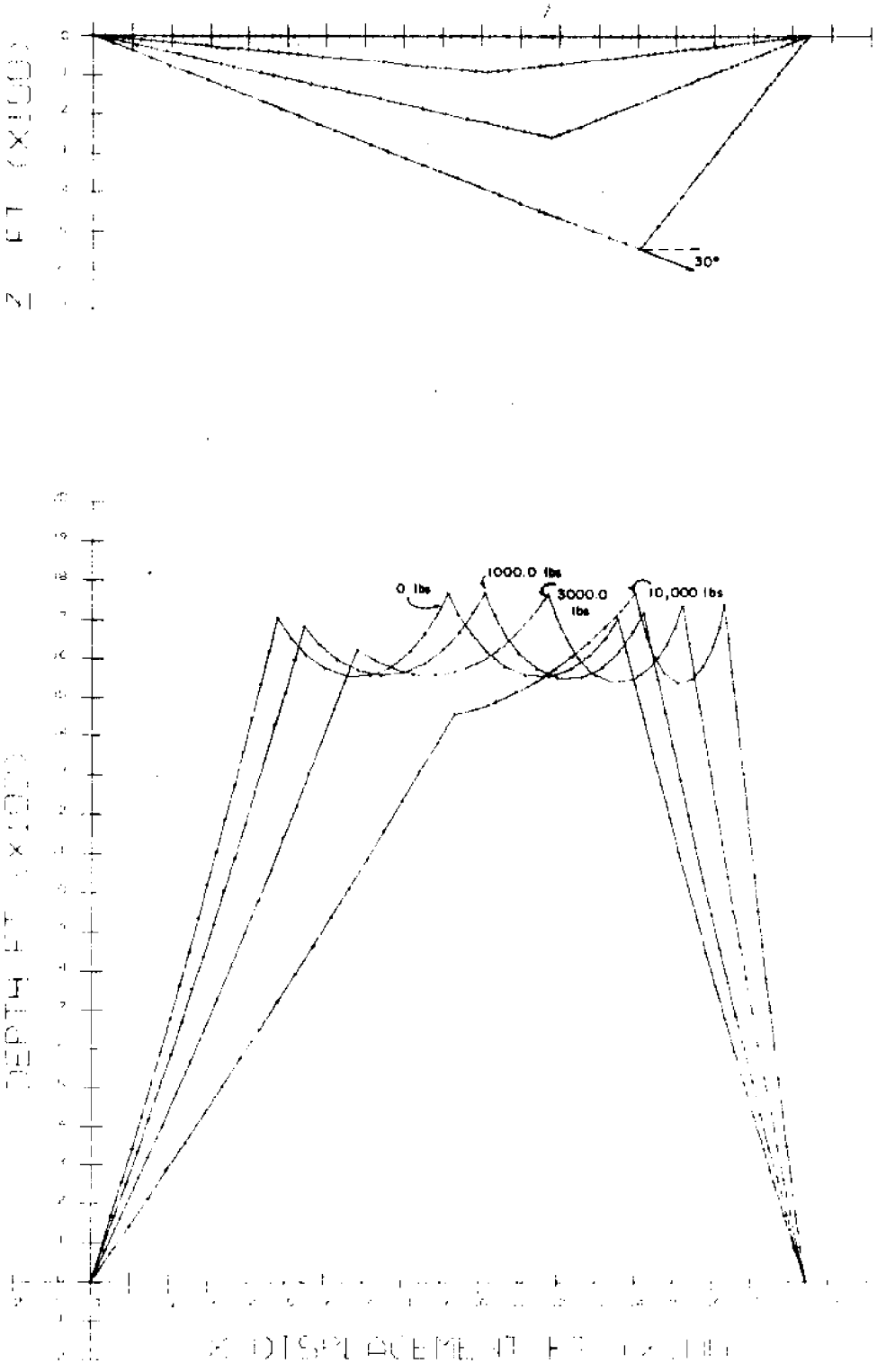

Figure 2.10-3 MOORING GEOMETRY FOR SURFACE LOADS AT θ = 30°

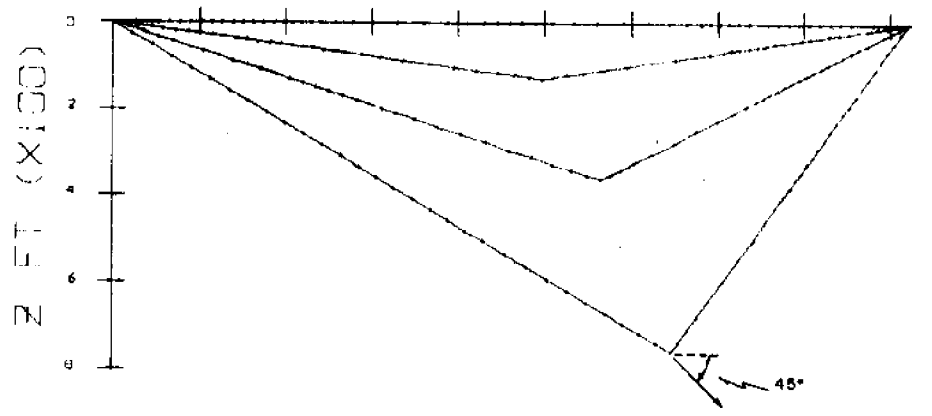

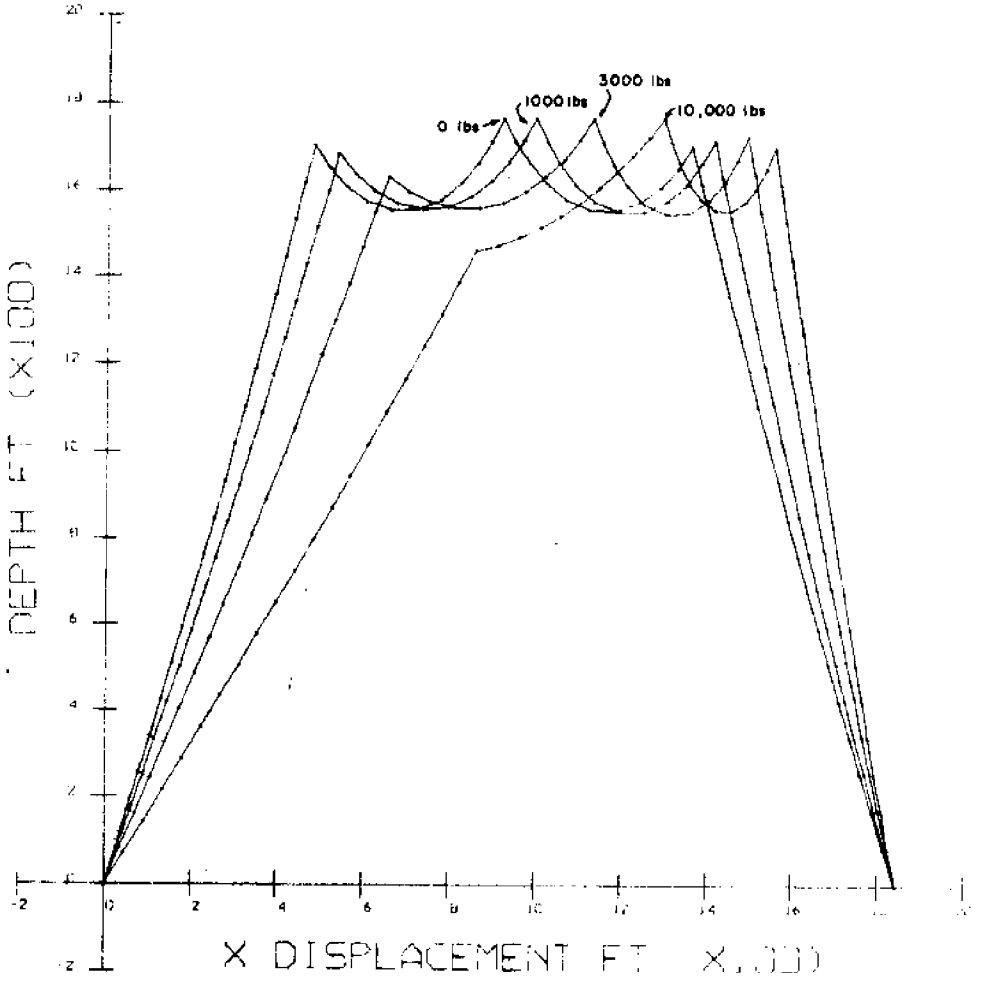

Figure 2.10-4 MOORING GEOMETRY FOR SURFACE LOADS AT θ = 45°

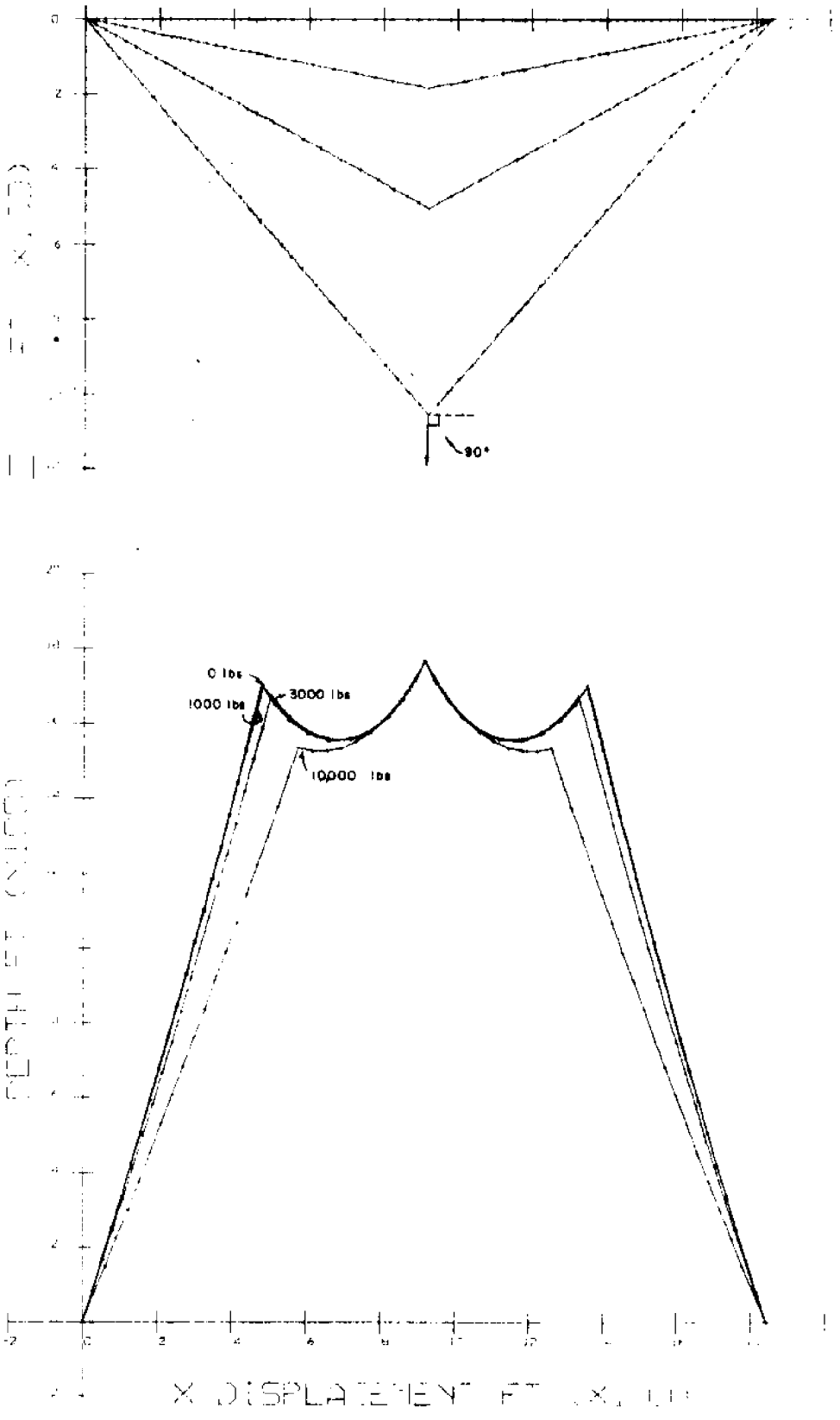

Figure 2.10-5 MOORING GEOMETRY FOR SURFACE LOADS AT θ = 90°

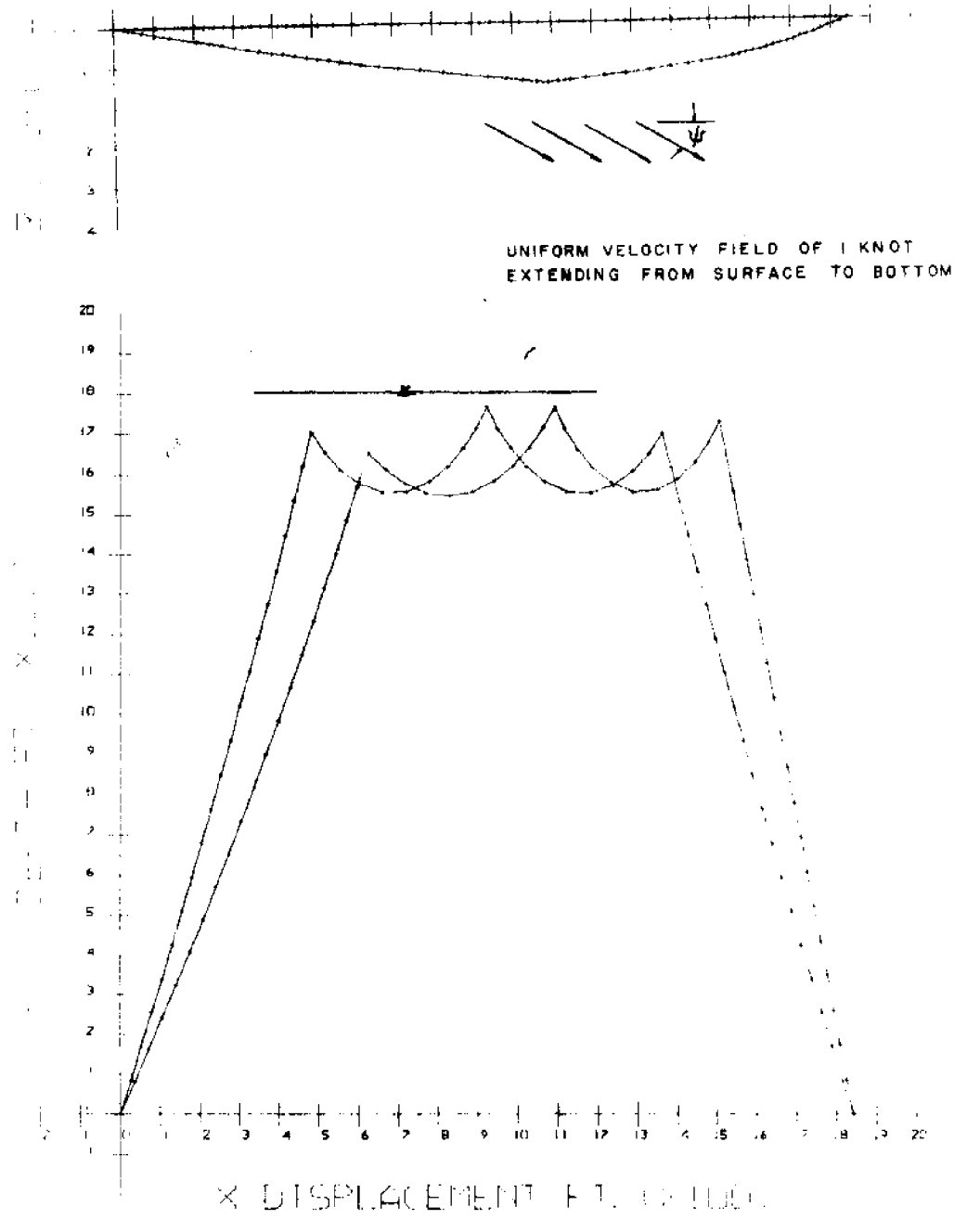

Figure 2.10-6 MOORING GEOMETRY FOR COMBINED SURFACE AND SUBSURFACE LOADINGS

2.11. Discussion

Accuracy which is achievable exceeds that normally required and appears limited only by the number of cable segments utilized. Use of a large number of segments, though probably seldom necessary, is not prohibitive. When using a discrete cable system model, a greater number of segments should be incorporated in cables having a negative σ ratio than those which are positive, if consistent tension accuracy is to be achieved throughout the system. Hydrodynamic forces on subsurface elements can be significant, and should be accounted for, as their neglect can lead to appreciable error.

Once basic computer programs have been developed, the discrete parameter formulation provides direct transition to dynamic analysis (Dominguez 1971).

The use of a discrete parameter model, in conjunction with a high speed digital computer, results in a powerful tool for arriving at statical solutions to complicated cable analysis problems. Experience has shown it to be versatile and highly efficient. Basic programs can be written to readily accommodate analysis of different systems, making it a practical technique for design applications.

BIBLIOGRAPHY

Dominguez, Richard F. et al. 1969. Analysis of a two-point mooring for a spar buoy. (Oregon State University. Dept. of Oceanography. Data Report No. 38, Reference 69-34)

Dominguez, Richard F. 1971. The static and dynamic analysis of discretely represented moorings and cables by numerical means. Ph.D. dissertation. Corvallis, Oregon State University. 143 numb. leaves.

Michalos, James and Charles Birnstiel. 1962. Movements of a cable due to changes in loading. Part II. Transaction of the American Society of Civil Engineers 127:267-303.

Michalos, James and Edward N. Wilson. 1965. Structural Mechanics and Analysis. New York, The Macmillan Company, 430 p.

O'Brien, Terence. 1967. General solution of suspended cable problems. Journal of the Structural Division, American Society of Civil Engineers, Proc. Paper 5085, No. ST1, 93:1-26.

O'Brien, W. Terrence and Arthur J. Francis. 1964. Cable movements under two-dimensional loads. In: Journal of the Structural Division, Proceedings of the American Society of Civil Engineers, Ann Arbor, Michigan. No. ST1, Part 1, 90:89-123.

Parsons, Micheal G. and Mario J. Casarella. 1969. A survey of studies on the configuration of cable systems under hydrodynamic loading. 86 numb. leaves. (The Catholic University of America. Dept. of Mechanical Engineering. Report 69-1 Themis Program No. 893 (1968-1971) N00014-68-A-0506-0001.)

Pestel, Eduard C. and William T. Thomson. 1969. Statics. New York, McGraw-Hill. 400 p.

Shore, Sidney (comp.) 1969. Bibliography - structural applications of steel cable systems. New York, American Iron and Steel Institute. 28 p.

Skop, R. A. and G. J. O'Hara. 1969. The static equilibrium configuration of cable arrays by use of the method of imaginary reactions. 36 numb. leaves. (Naval Research Laboratory. Ocean Structures Branch. Ocean Technology Division. Washington, D.C. NRL Report 6819.)

Wilson, B.W. 1967. Elastic characteristics of moorings. Journal of the Waterways and Harbors Division, Proceedings of the American Society of Civil Engineers 93, WW4:27-56. Nov. 1967.